XIII International Conference on Gravitation, Astrophysics & Cosmology – 15th Italian-Korean Symposium on Relativistic Astrophysics - A joint meeting

Ewha Womans University,

July 7, 2017, Seoul, Korea

"What can we learn from GRBs?"

Marco Muccino

University of Rome "Sapienza" & ICRANet, Italy

On behalf of a large collaboration

R. Ruffini, Y. Aimuratov, L.M. Becerra, C.L. Bianco, C. Cherubini, S. Filippi, C.L. Fryer, M. Karlica, M. Kovacevic, D.J. Melon Fuksman, R. Moradi, A.V. Penacchioni, G.B. Pisani, D. Primorac, J.F. Rodriguez, J.A. Rueda, S. Shakeri, G. Vereshchagin, Y. Wang & S.-S. Xue

GRB classification: a forensic investigations

$E_{p,i}$-E_{iso} relations for short and long bursts [1–5]

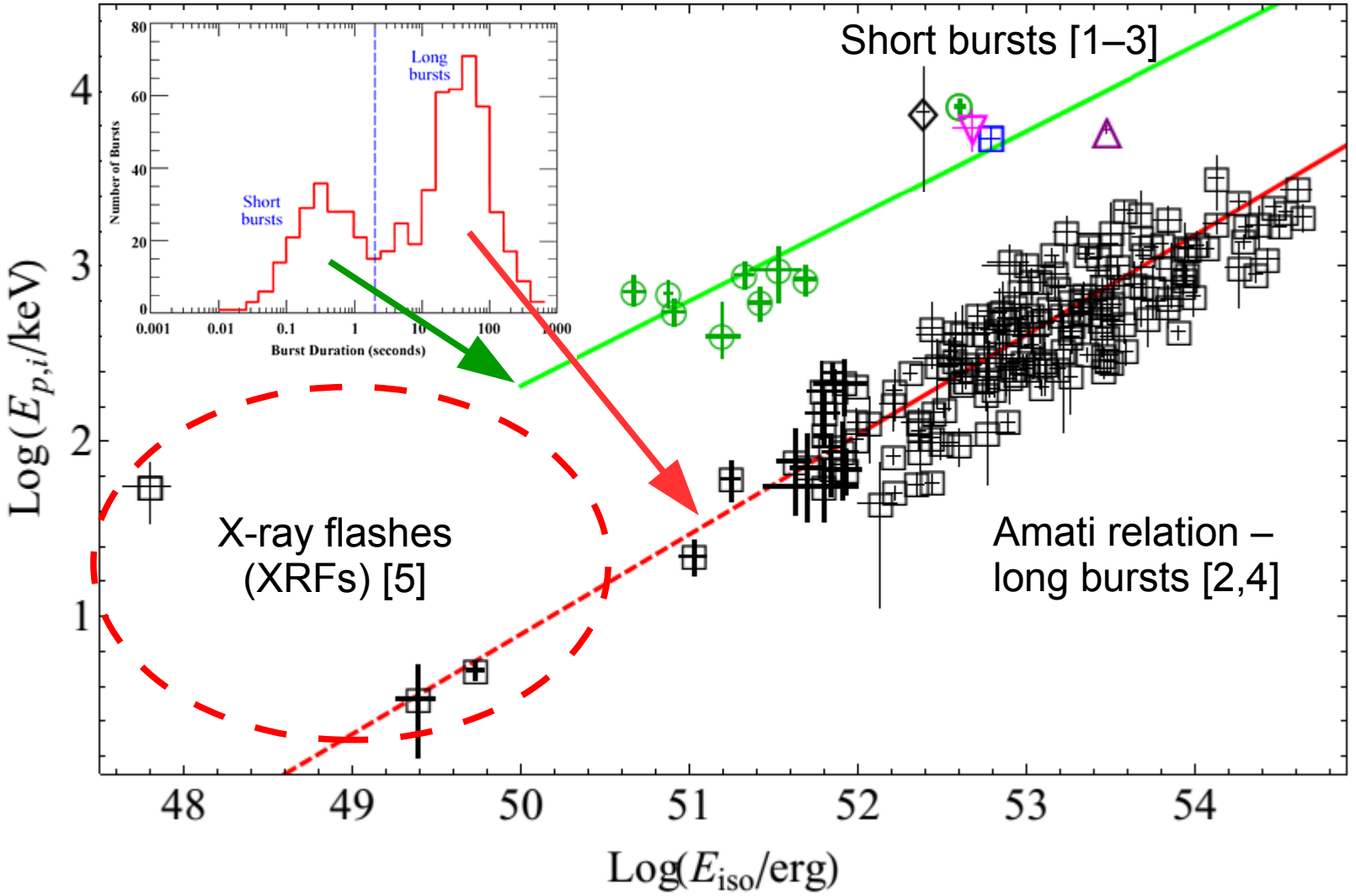

Is the classification really that simple?

Is this as much one can extract from γ-rays and what about other energy bands?

[1] Zhang, F.-W., Shao, L., Yan, J.-Z., & Wei, D.-M. 2012, ApJ, 750, 88.
[2] Calderone, G., Ghirlanda, G., Ghisellini, G., et al. 2015, MNRAS, 448, 403.
[3] Ruffini, R., Rueda, J.A., Muccino, M., et al. 2016 ApJ, 832, 136
[4] Amati, L., & Della Valle, M. 2013, International Journal of Modern Physics
[5] Soderberg, A. M., Kulkarni, S. R., Nakar, E., et al. 2006, Nature, 442, 1014

GeV emission for short and long bursts [6–9]

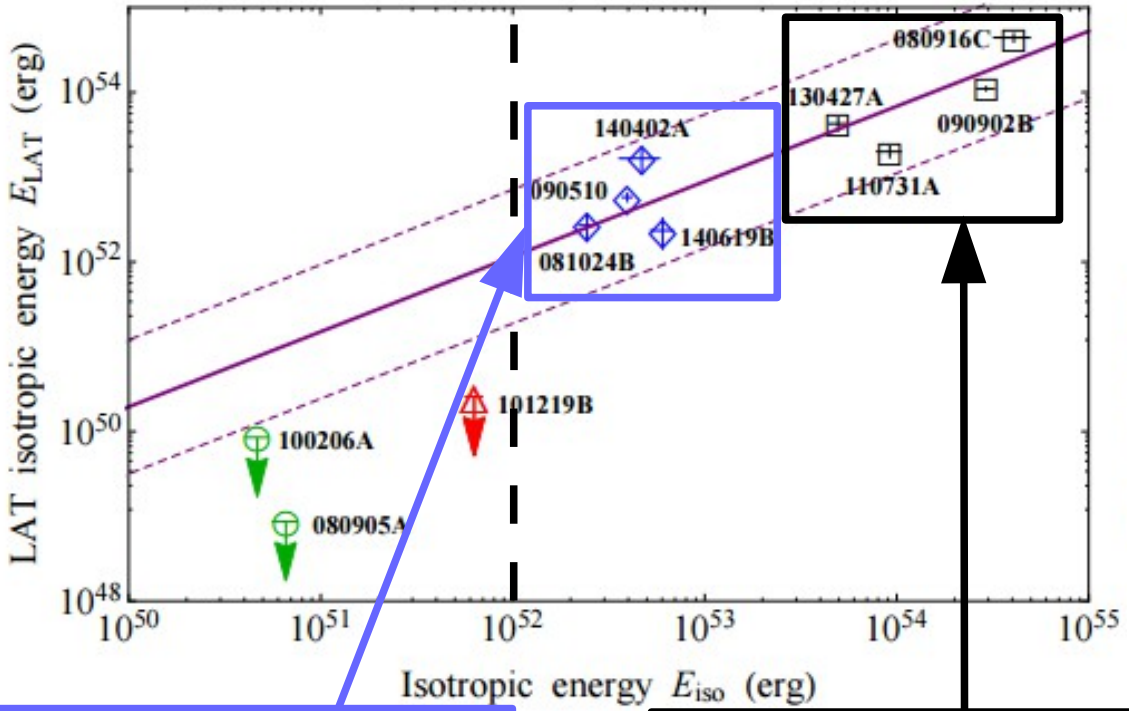

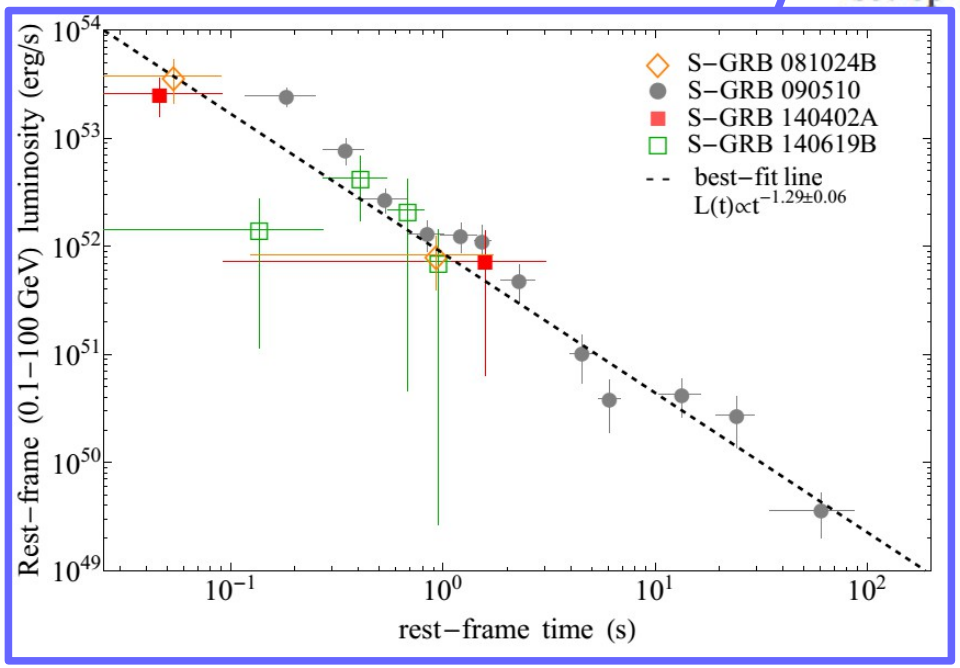

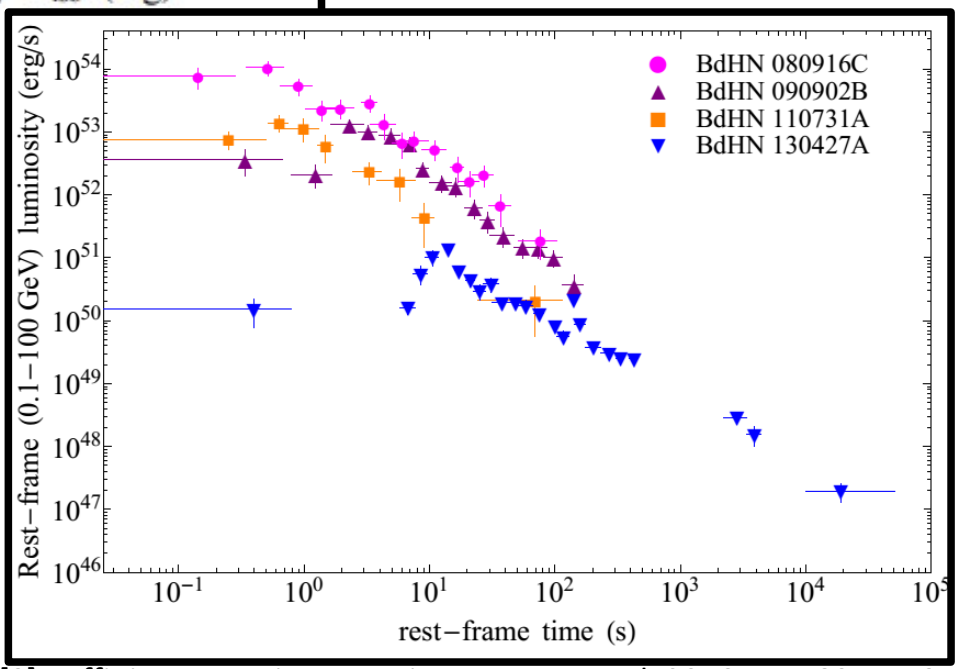

[6] Ruffini, R., Wang, Y., Enderli, M., et al. 2015a, ApJ, 798, 10
[7] Ruffini, R., Muccino, M., Kovacevic, M., et al. 2015, ApJ, 808, 190
[8] Ruffini, R., Muccino, M., Aimuratov, Y., et al. 2016, ApJ, 831, 178
[9] Aimuratov, Y., Ruffini, R., et al., 2017, arXiv:170408179A

X-ray emission for short and long bursts

$< 10^{52}$ erg

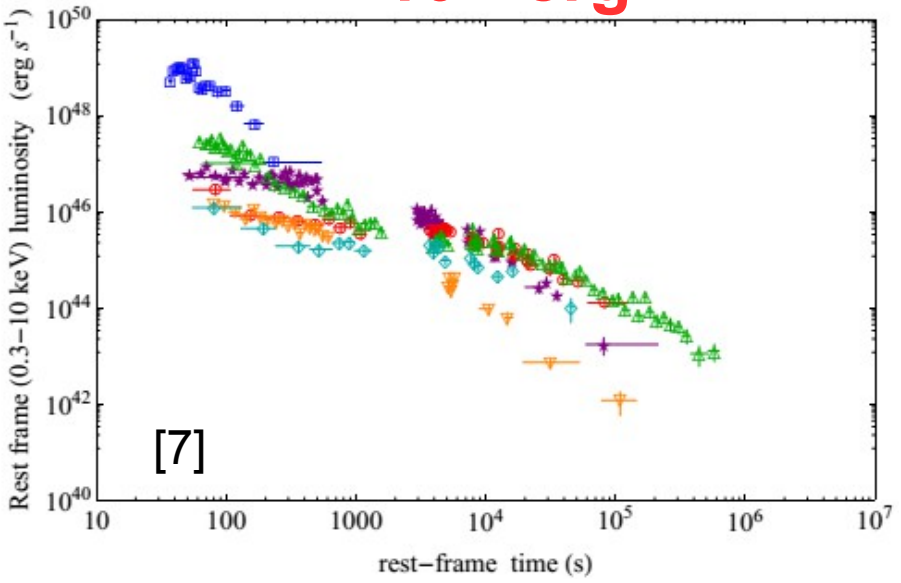

short bursts

$> 10^{52}$ erg

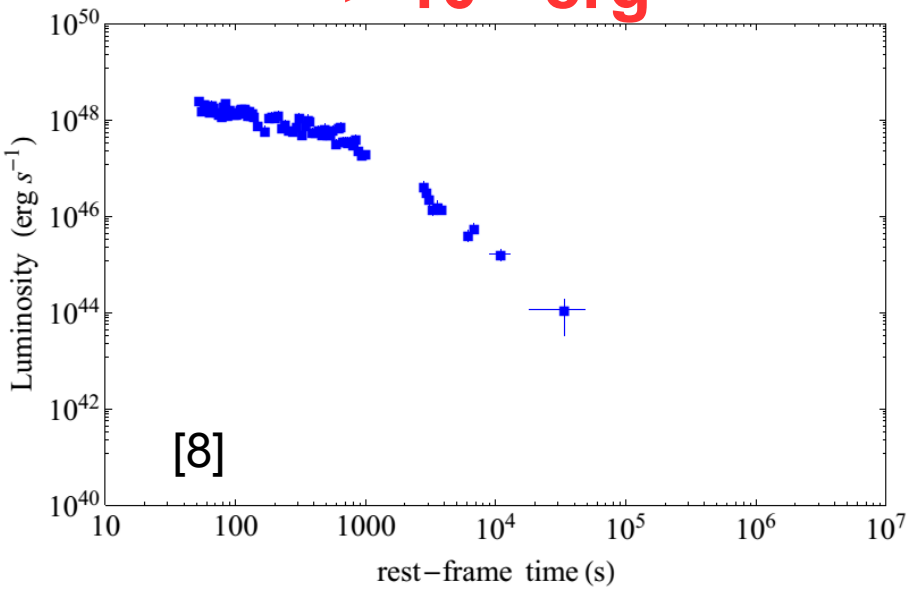

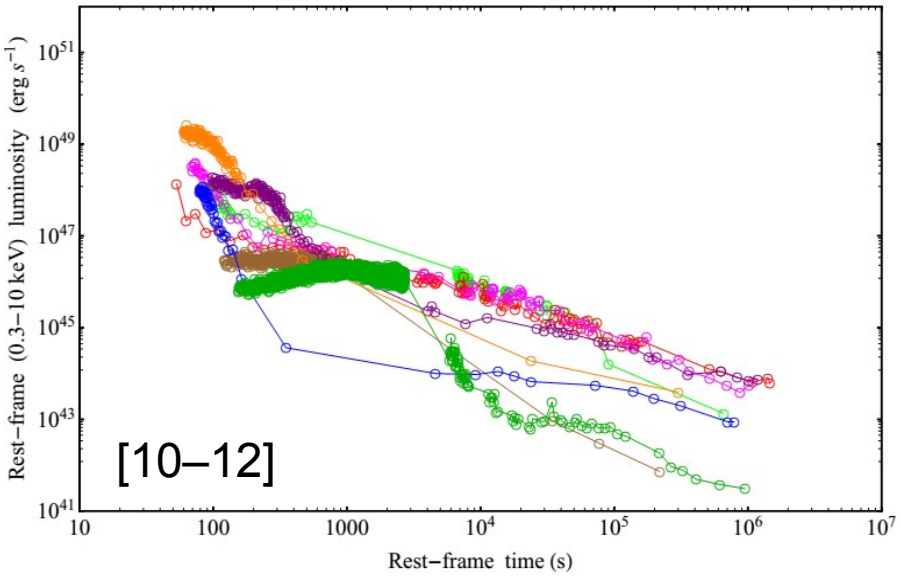

long bursts

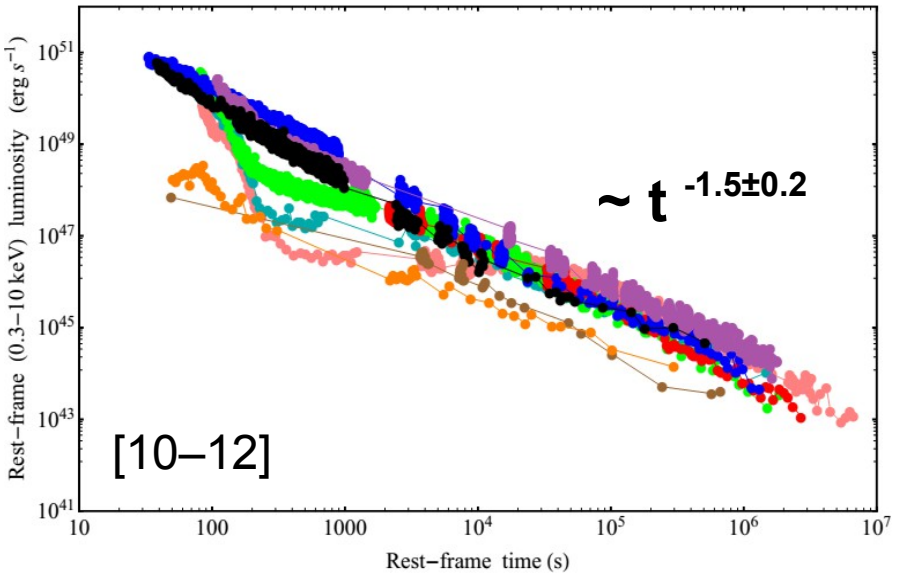

[10] Pisani, G. B., Izzo, L., Ruffini, R., et al. 2013, A&A, 552, L5
[11] Pisani, G. B., Ruffini, R., Aimuratov, Y., et al. 2016, ApJ, 833, 159
[12] Ruffini, R., Wang, Y., Aimuratov, Y., et al 2017, arXiv:170403821

$E_{p,i}$-E_{iso} relations for short and long GRBs [3]

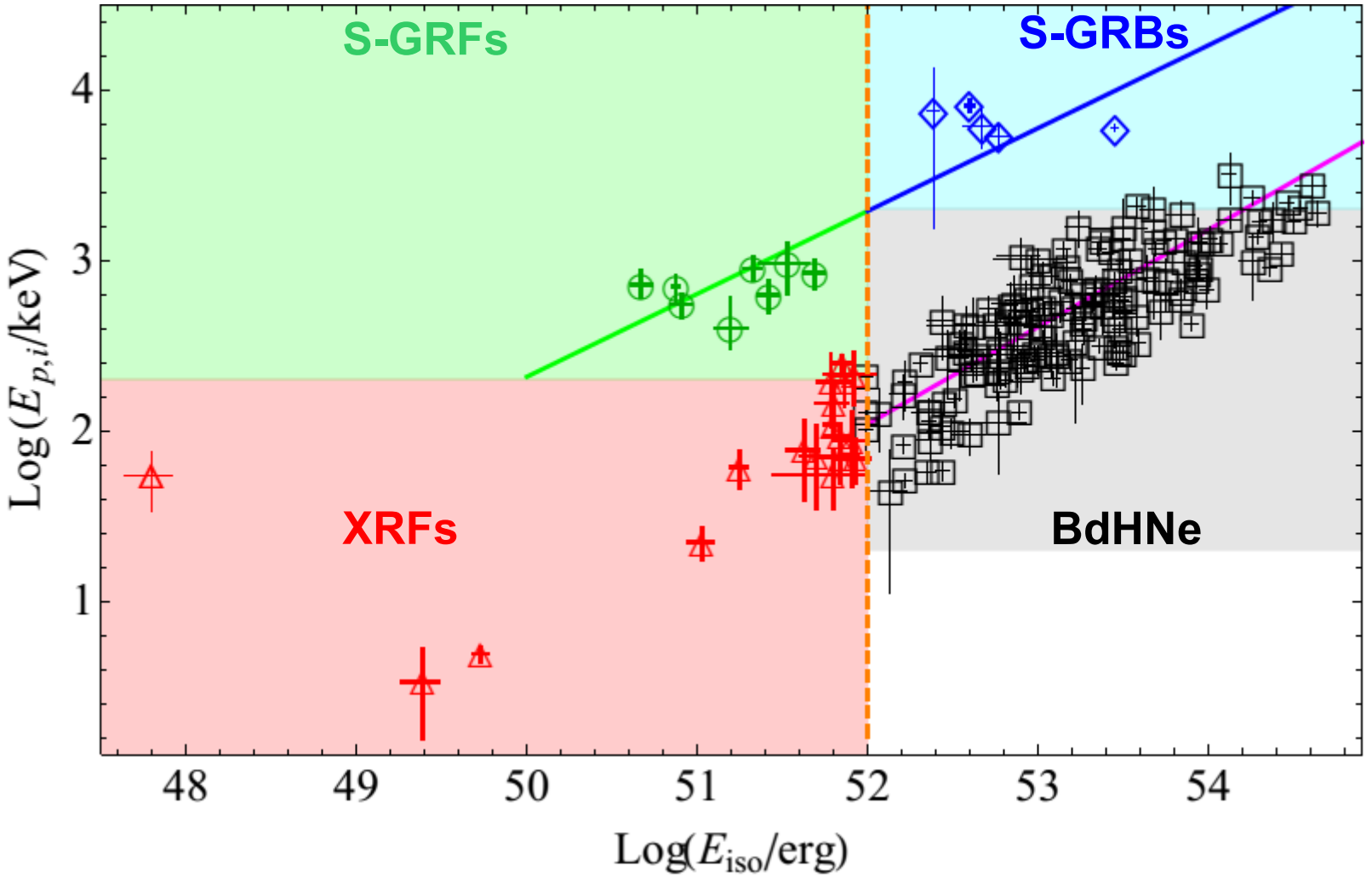

– S-GRF = short gamma-ray flash;
– S-GRB = authentic short GRB;
– XRF = X-ray flash;
– BdHN = binary-driven hypernova.

[3] Ruffini, R., Rueda, J.A., Muccino, M., et al. 2016 ApJ, 832, 136

The Induced Gravitational Collapse paradigm:

XRFs vs BdHNe

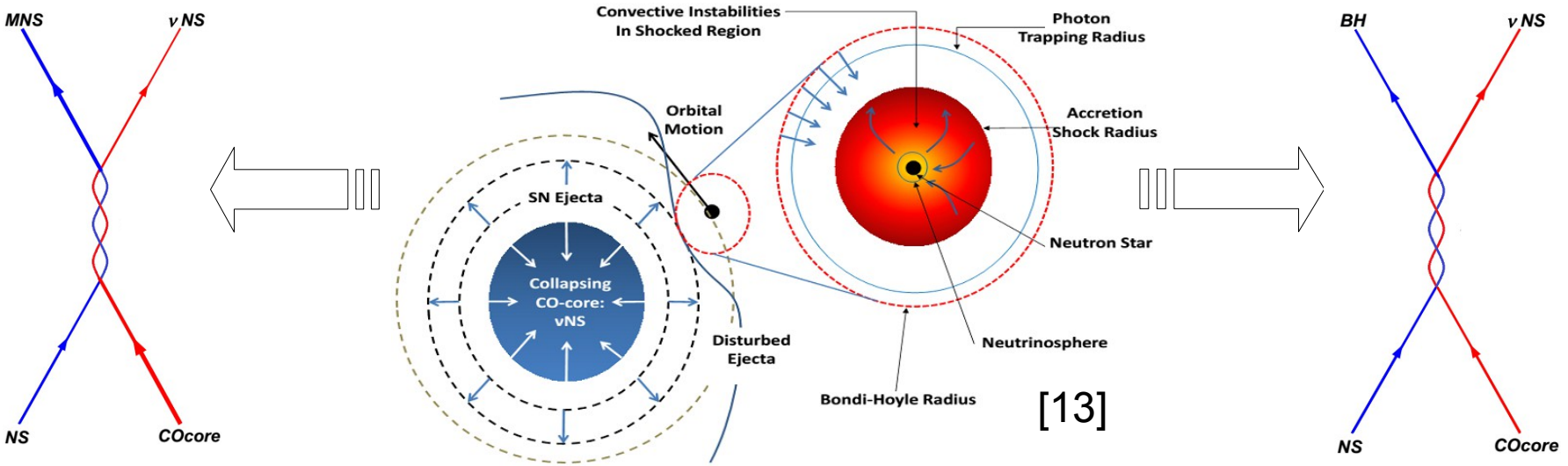

[13] Fryer, C. L., Rueda, J. A., & Ruffini, R. 2014, ApJ, 793, L36

The Induced Gravitational Collapse paradigm:

XRFs vs BdHNe

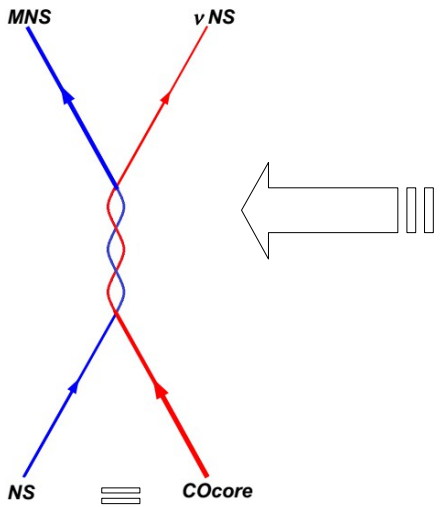

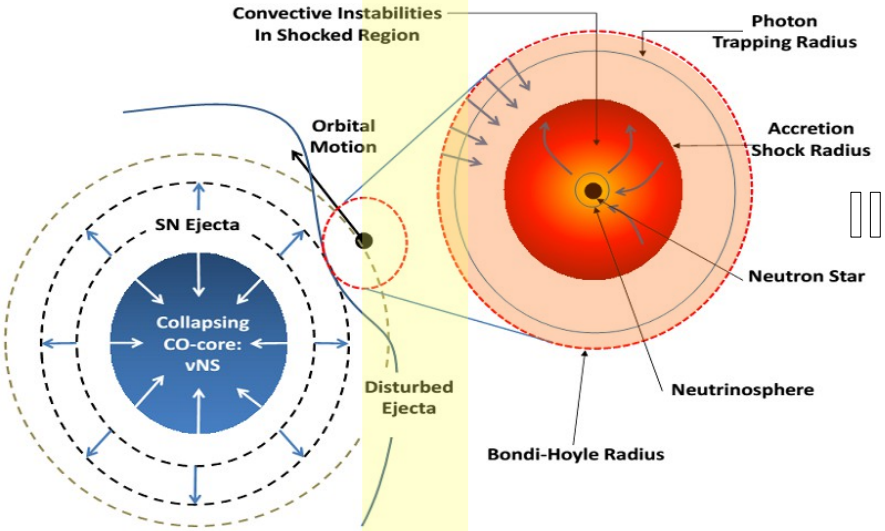

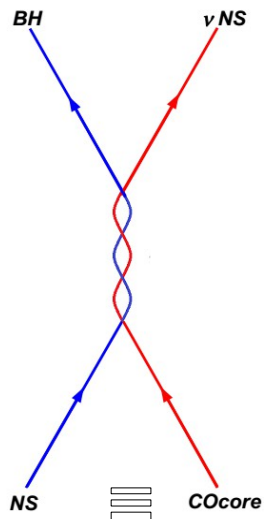

The hypercritical accretion phase

Episode 1:

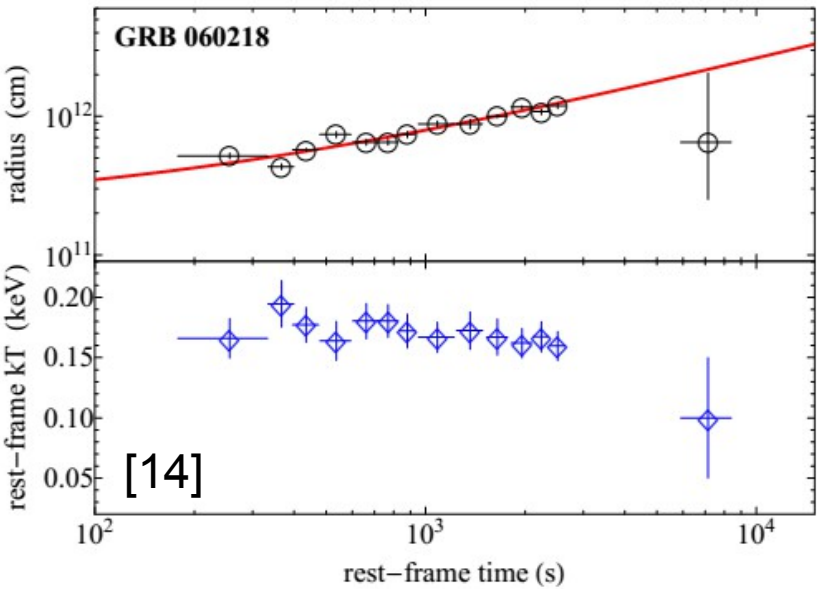

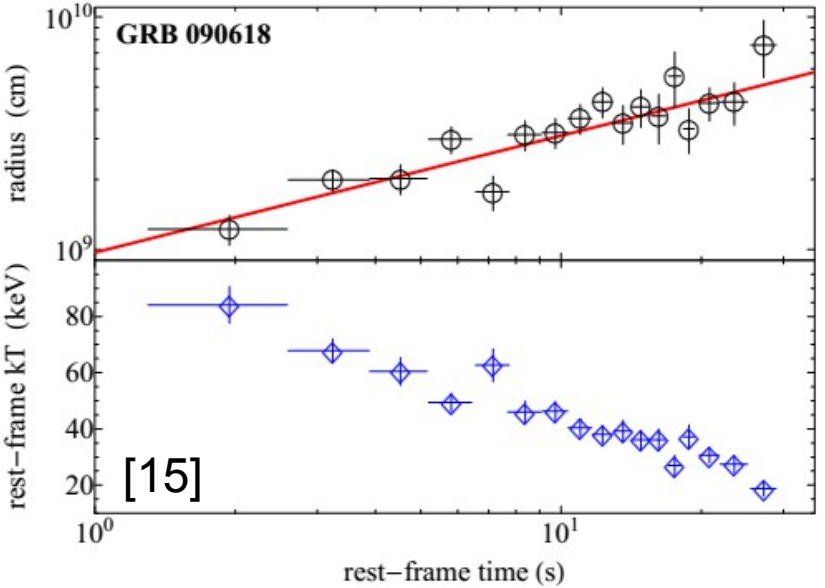

[14] Campana, S., Mangano, V., Blustin, A. J., et al. 2006, Nature, 442, 1008

[15] Izzo, L., Ruffini, R., Penacchioni, A. V., et al. 2012, A&A, 543, A10

The Induced Gravitational Collapse paradigm:

XRFs vs BdHNe

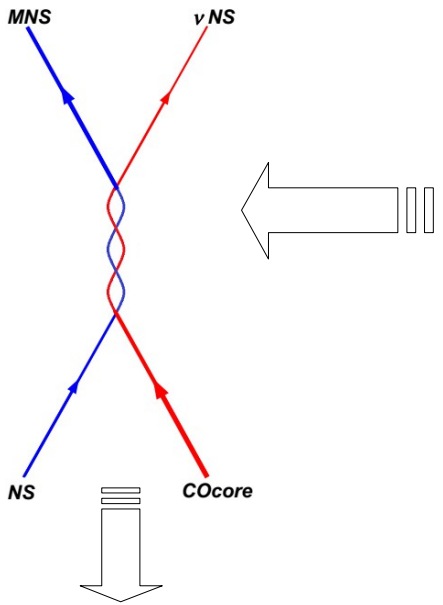

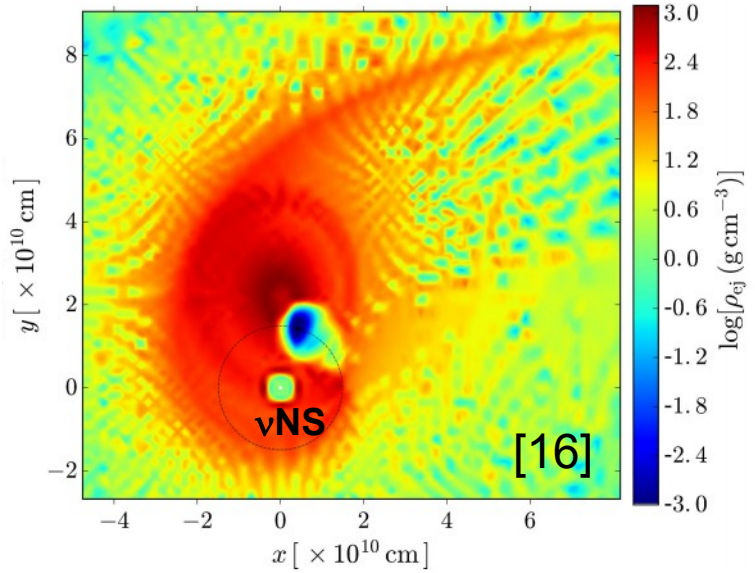

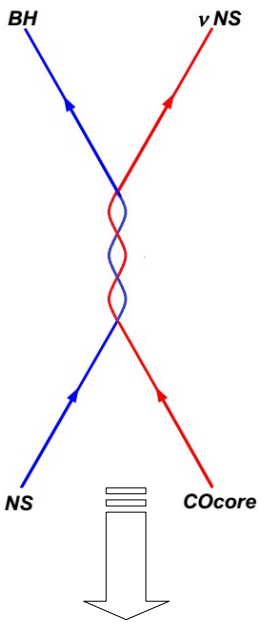

BH formation and GRB emission Episode 2:

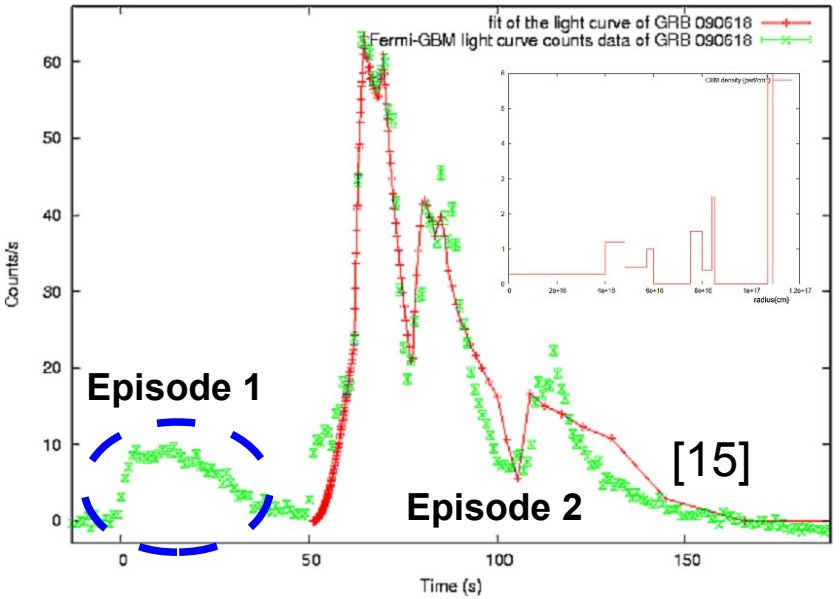

[16] Becerra, L., Bianco, C. L., Fryer, C. L., et al. 2016, ApJ, 833, 107

The Induced Gravitational Collapse paradigm:

XRFs vs BdHNe

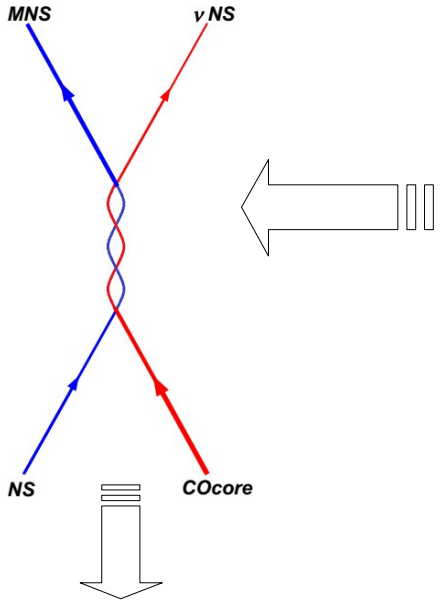

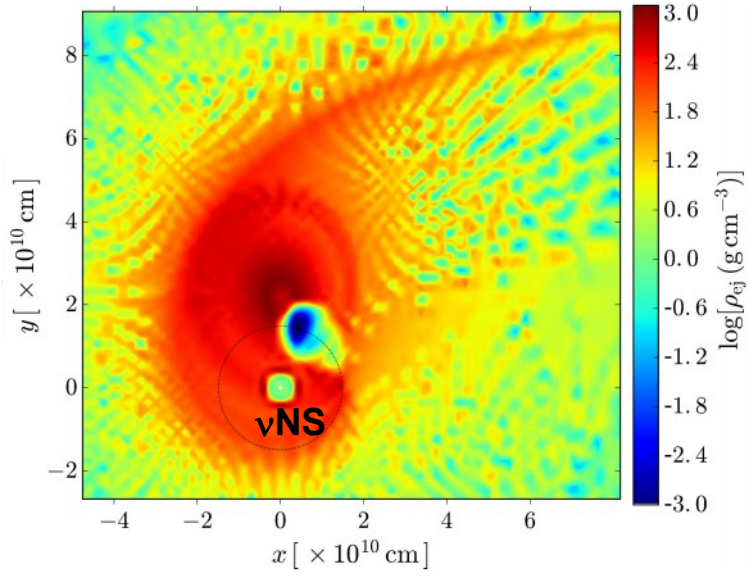

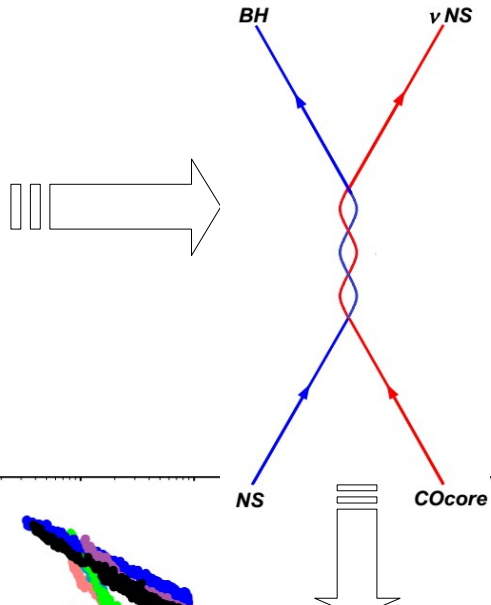

The X-ray flare-plateau-afterglow (FPA) phase:

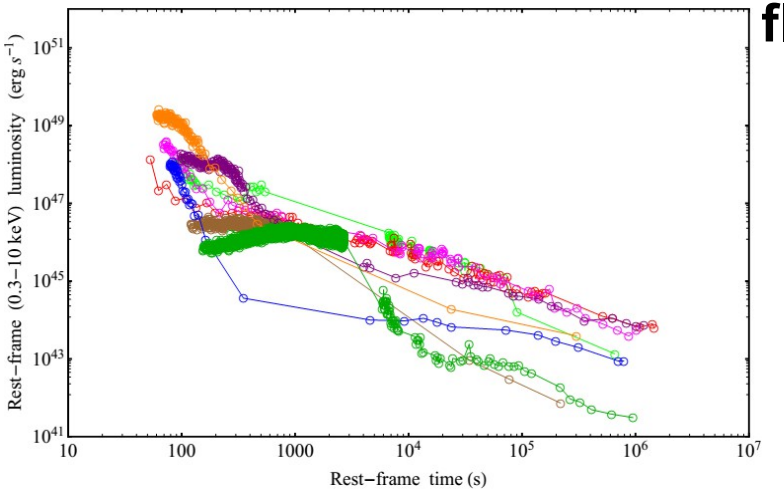

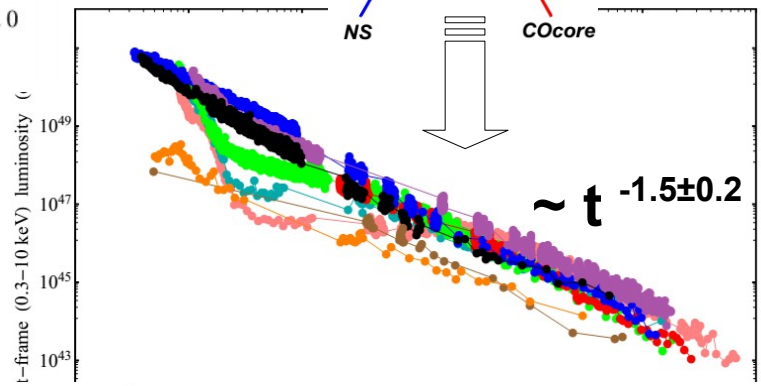

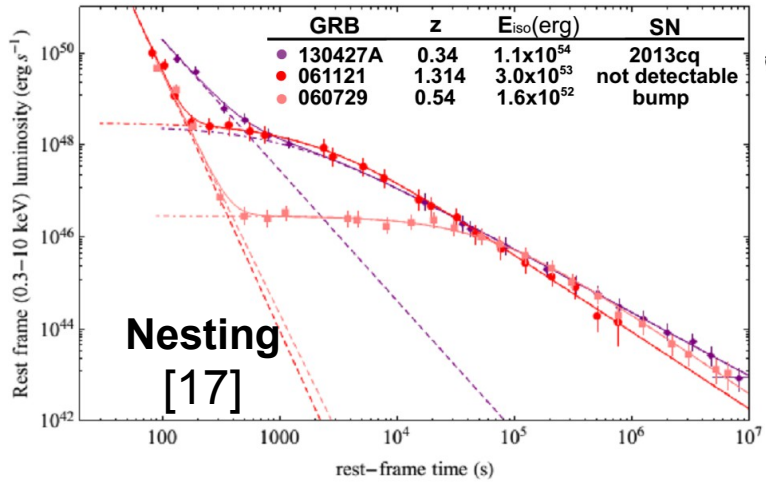

[17] Ruffini, R., Muccino, M., Bianco, C. L., et al. 2014, A&A, 565, L10

The FPA phase in BdHNe

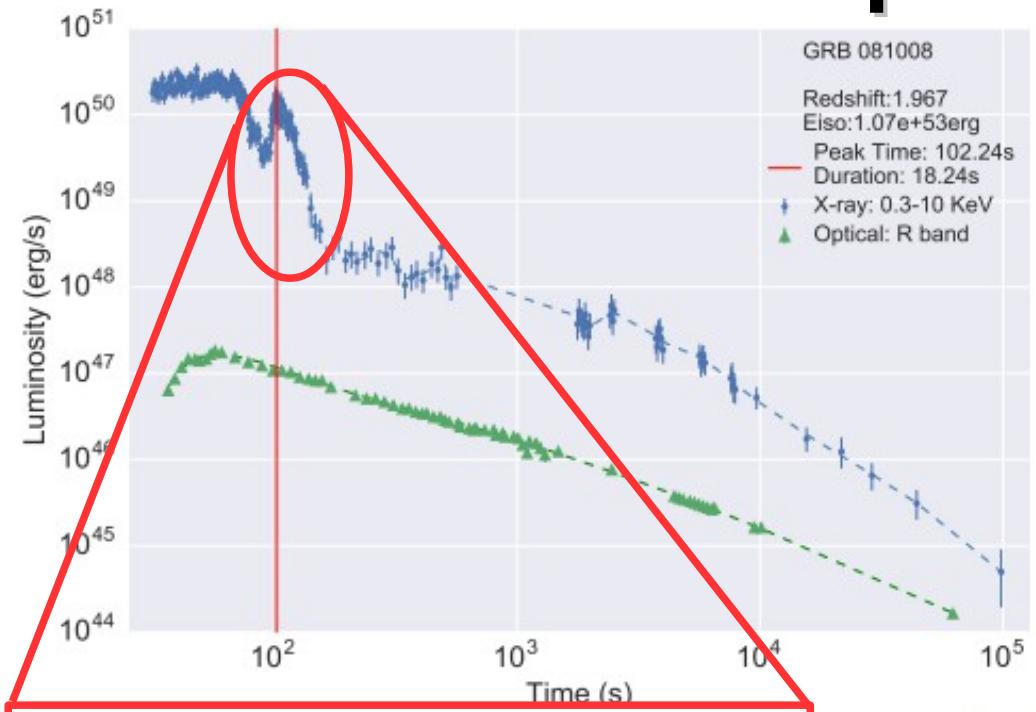

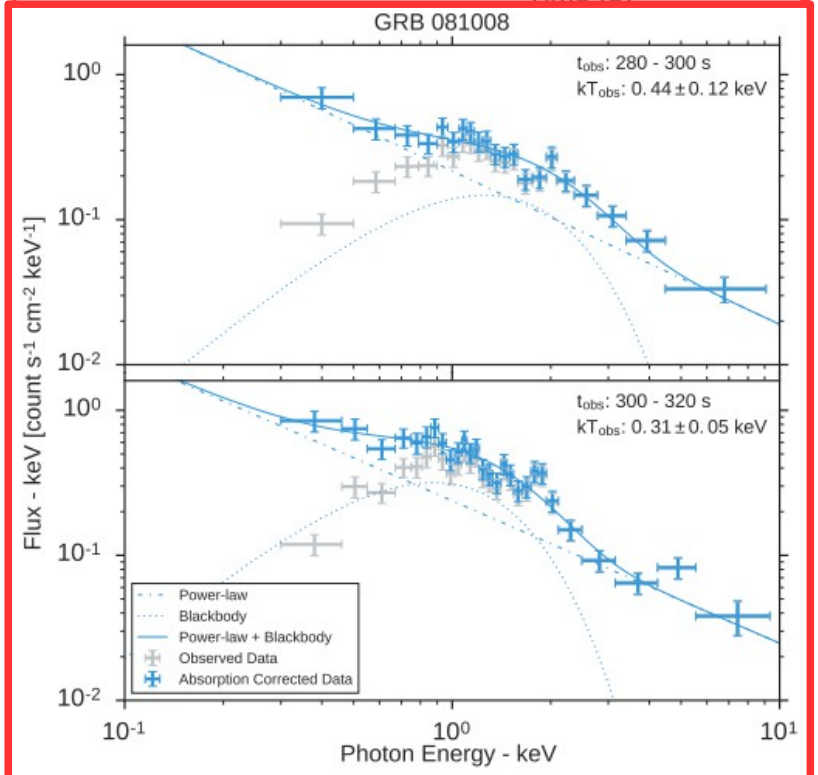

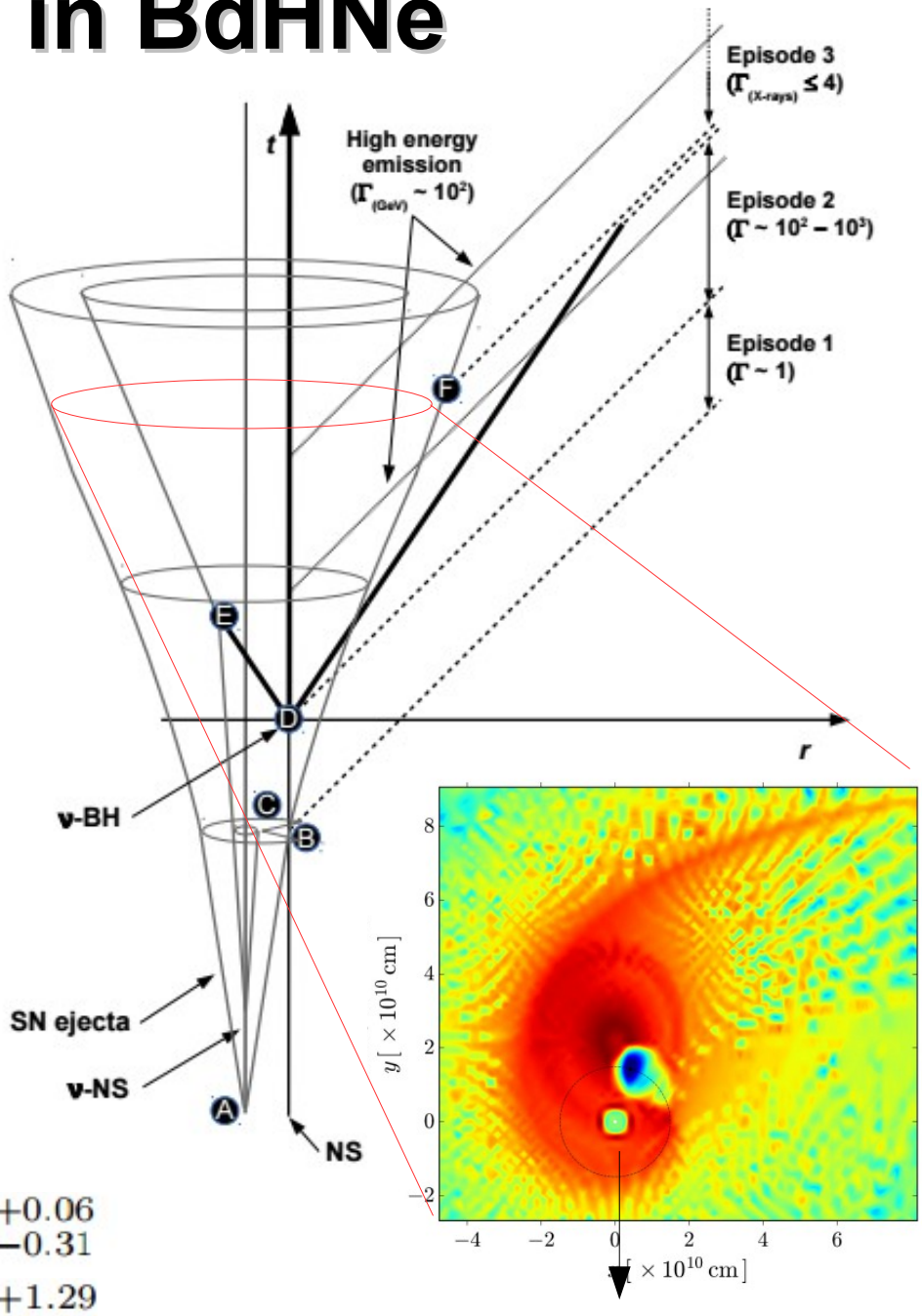

$$\langle \beta \rangle = 0.90^{+0.06}_{-0.31}$$

$$\langle \Gamma \rangle = 2.34^{+1.29}_{-1.10}$$

Ruffini, R., Wang, Y., Aimuratov, Y., et al 2017, arXiv:170403821

The Induced Gravitational Collapse paradigm:

XRFs vs BdHNe

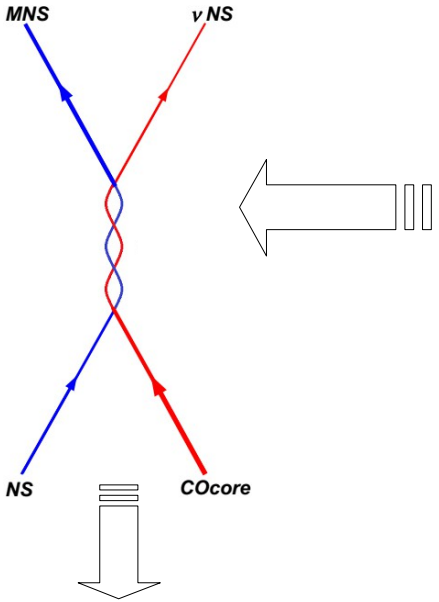

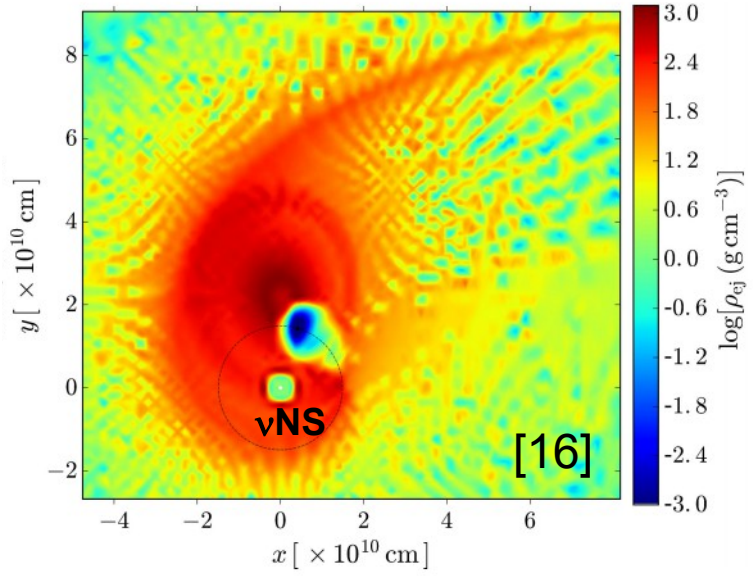

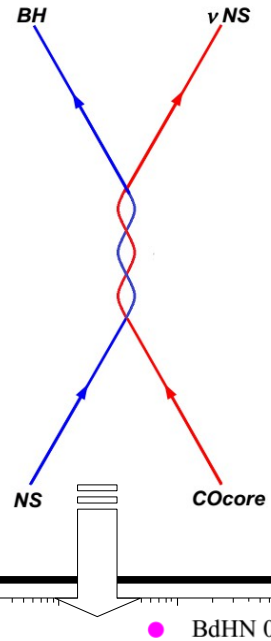

GeV emission:

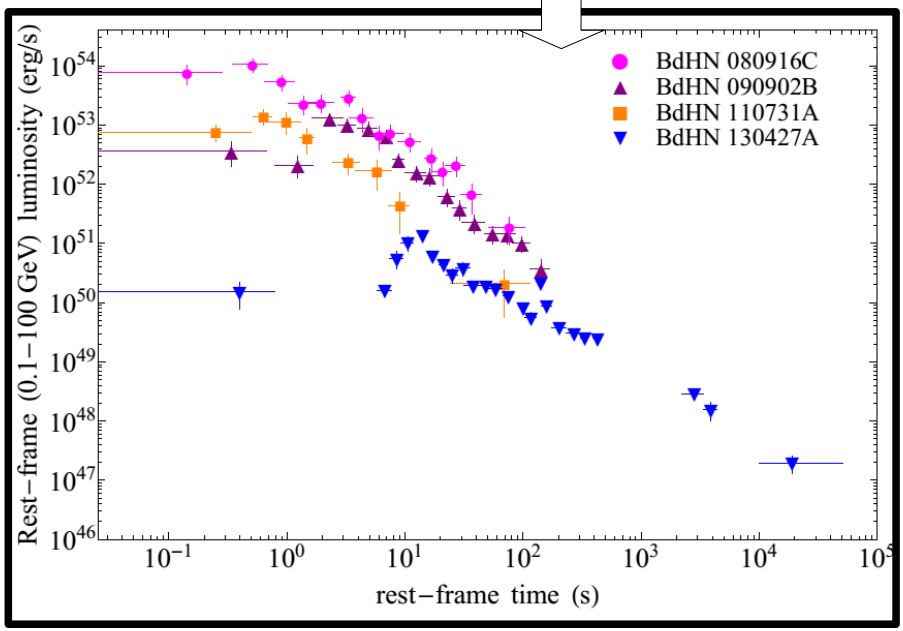

In the IGC paradigm the 0.1–100 GeV emission correlates with the BH formation and arises from the accretion process of matter bound to the new-born BH [3,6].

The merger paradigm:

S-GRFs vs S-GRBs

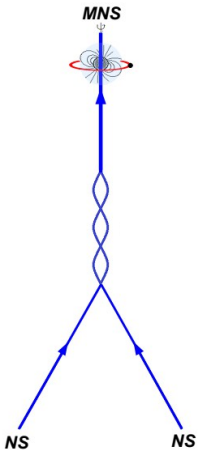

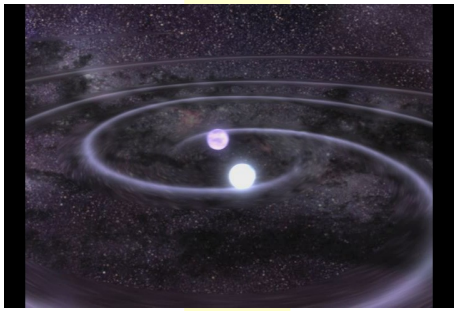

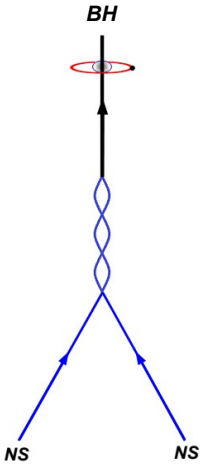

The merger paradigm:

S-GRFs vs S-GRBs

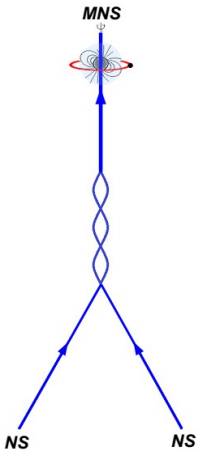

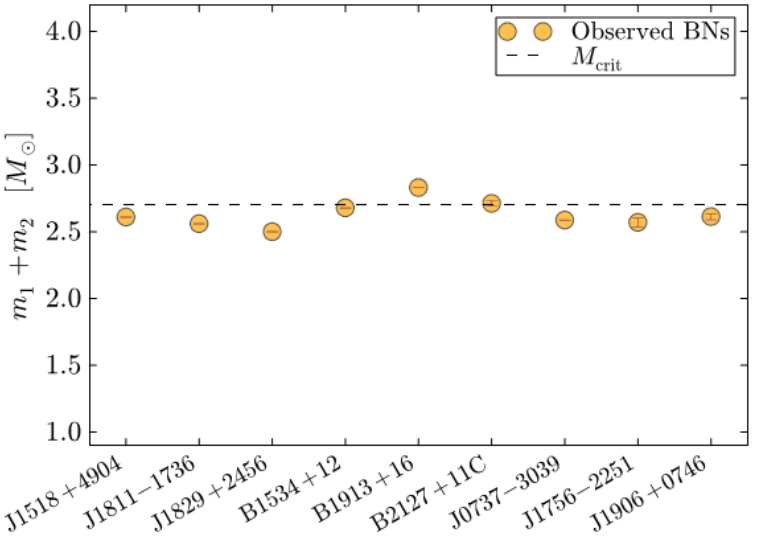

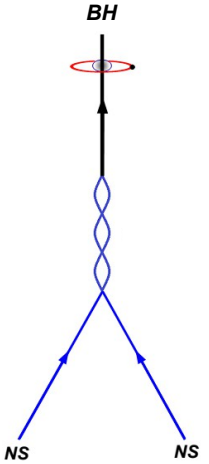

$\nu\bar{\nu} \rightarrow e^+e^-$? [18–19]

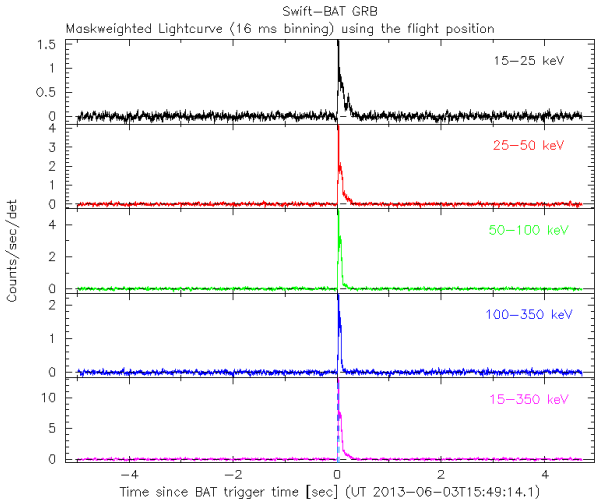

γ–ray emission:

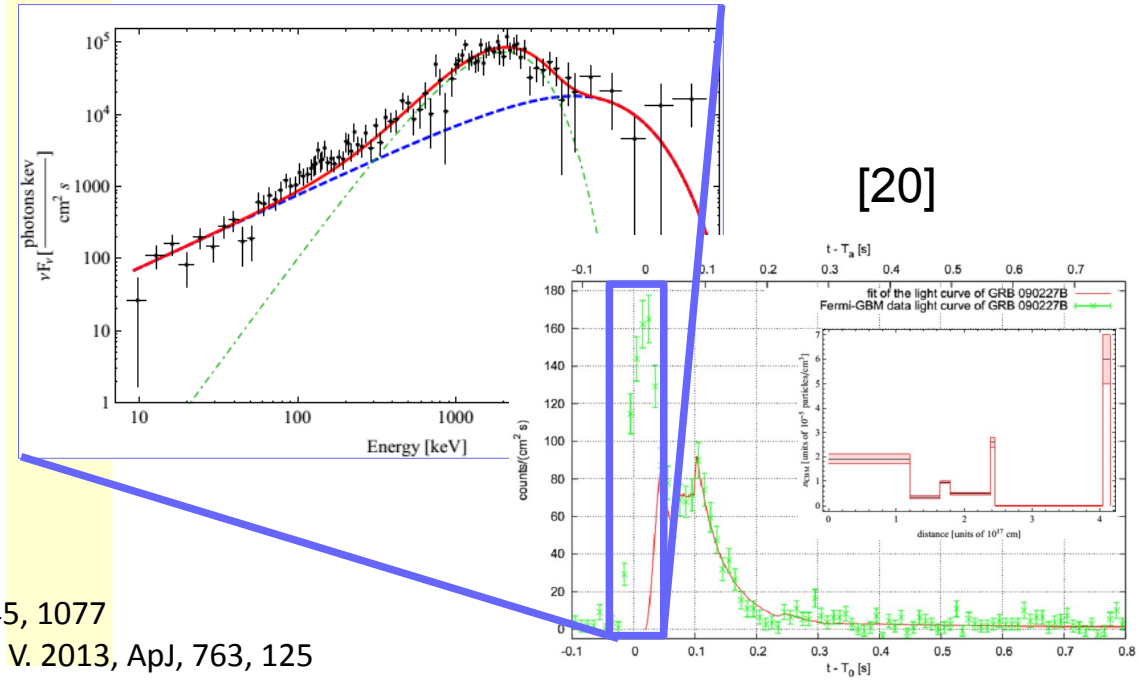

[20]

[18] Salmonson, J. D., & Wilson, J. R. 2002, ApJ, 578, 310

[19] Rosswog, S., Ramirez-Ruiz, E., & Davies, M. B. 2003, MNRAS, 345, 1077

[20] Muccino, M., Ruffini, R., Bianco, C. L., Izzo, L., & Penacchioni, A. V. 2013, ApJ, 763, 125

The merger paradigm:

S-GRFs vs S-GRBs

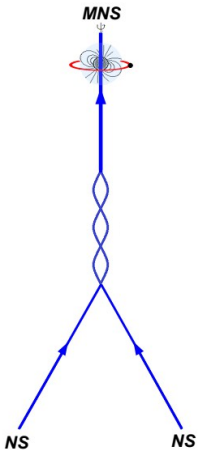

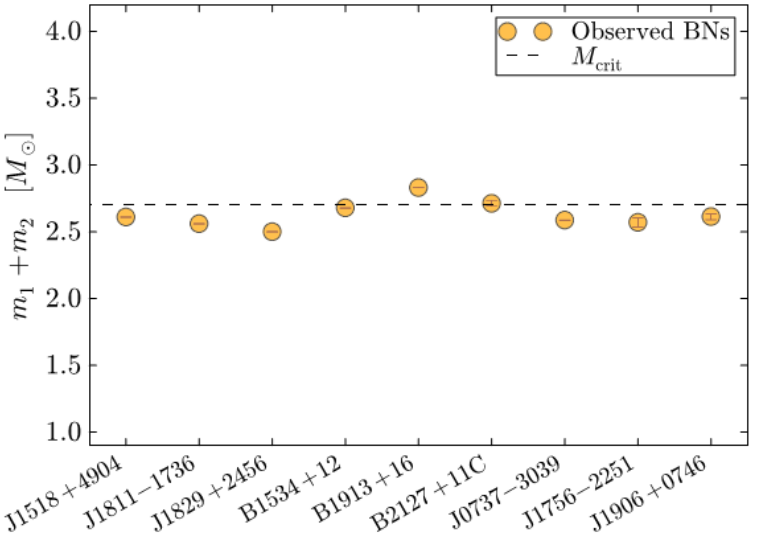

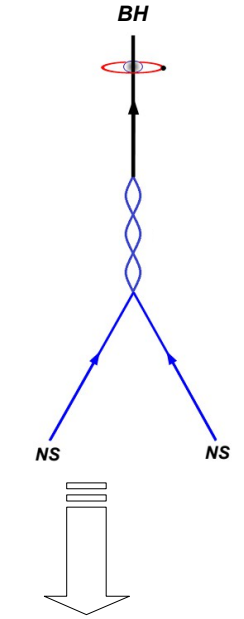

X-ray emission:

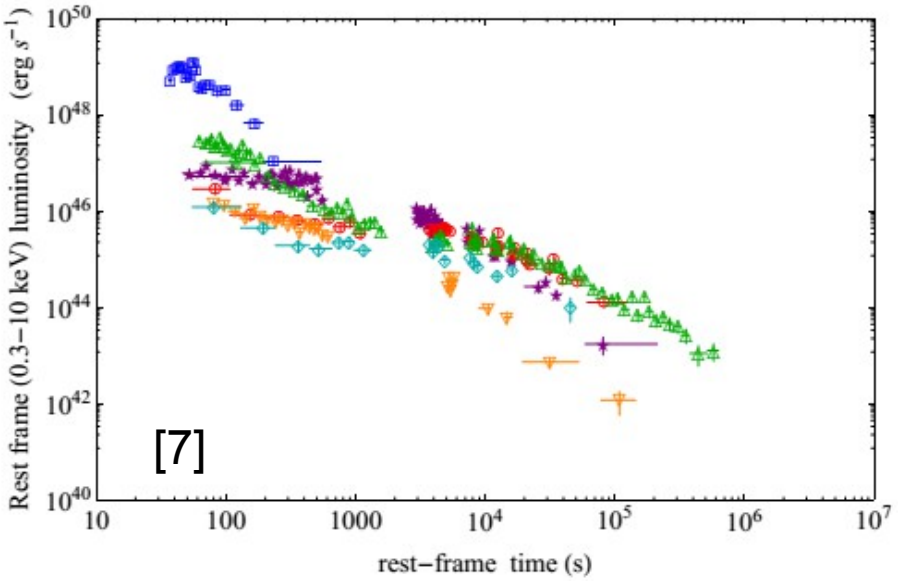

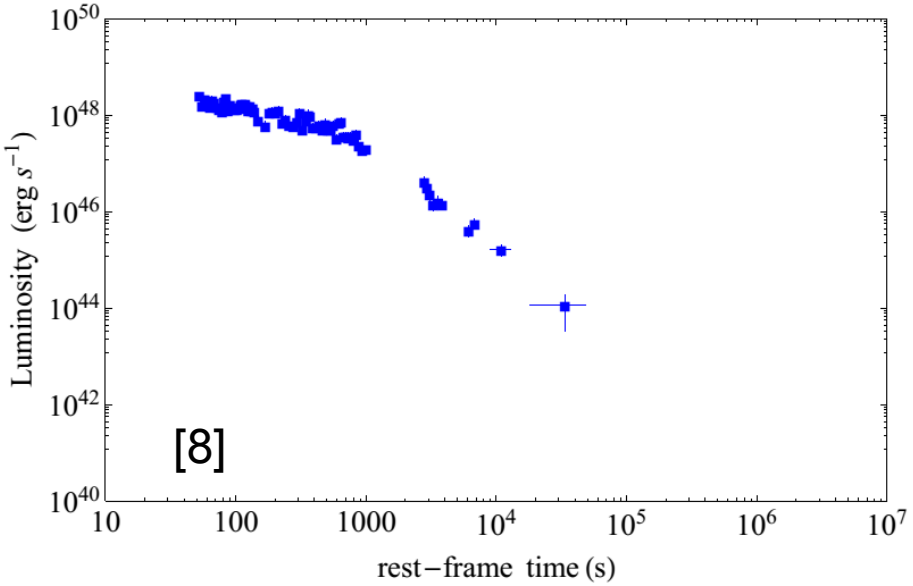

The merger paradigm:

S-GRFs vs S-GRBs

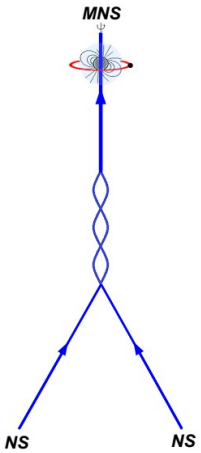

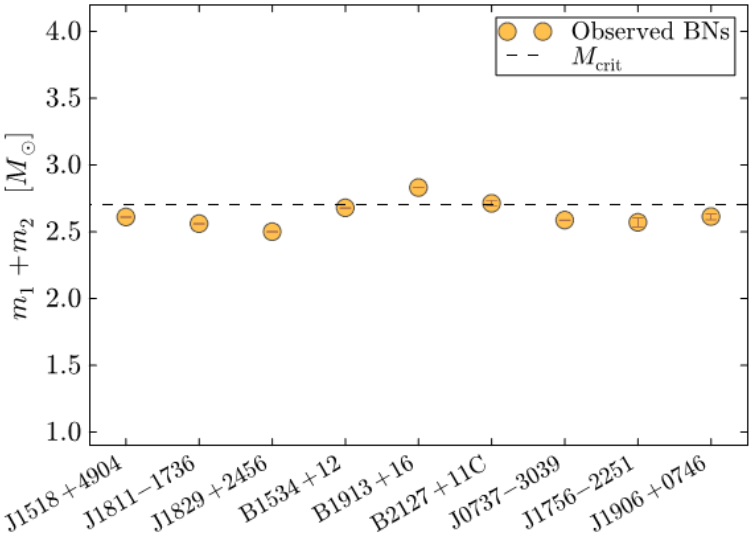

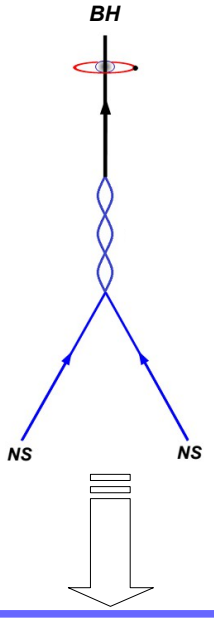

Gev emission:

it correlates with the BH formation and arises from the accretion of matter bound to the new-born BH [3,9].

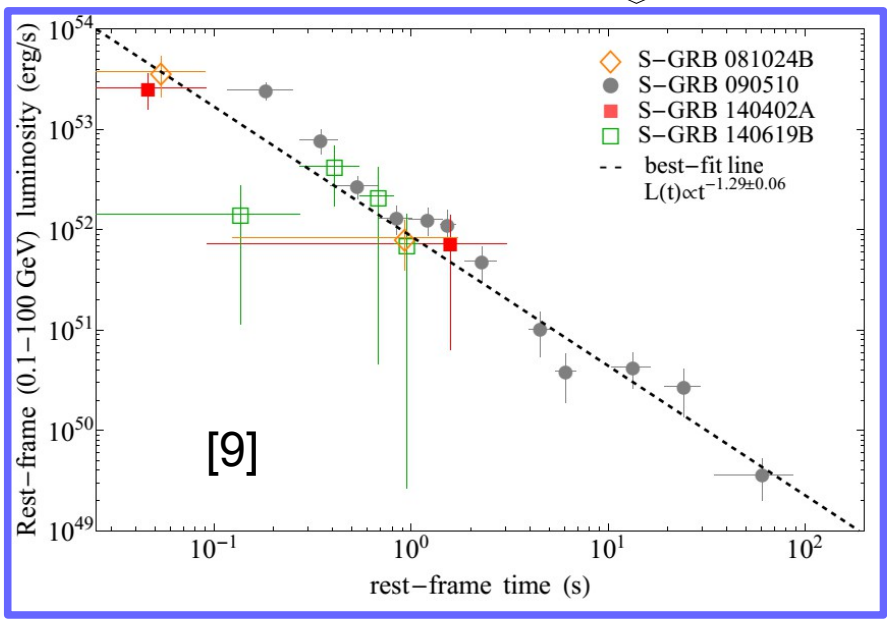

[9] Aimuratov, Y., Ruffini, R., et al., 2017, ApJ in press; arXiv:170408179

The 10^{52} erg lower limit in binary systems leading to BH formation

The total energy released during the hypercritical accretion process onto a NS is given by the gain of gravitational potential energy of the matter being accreted [3,21–25]:

$$L_{\rm acc} = \left(\dot{M}_b - \dot{M}_{\rm NS}\right) c^2 = \dot{M}_b c^2 \left[1 - \left(\frac{\partial M_{\rm NS}}{\partial J_{\rm NS}}\right)_{M_b} l - \left(\frac{\partial M_{\rm NS}}{\partial M_b}\right)_{J_{\rm NS}}\right]$$

Where

$$L_{\rm acc} \sim 0.1 \dot{M}_b c^2 \sim 10^{47}\text{–}10^{51}\ {\rm erg\ s^{-1}}$$

for

$$\dot{M}_b \sim 10^{-6}\text{–}10^{-2}\ M_\odot\ {\rm s^{-1}}$$

The lower limit of 10^{52} erg depends also on the yet unknown precise value of the NS critical mass

[21] Zel'dovich, Y. B., Ivanova, L. N., & Nadezhin, D. K. 1972, Soviet Ast., 16, 209.
[22] Ruffini, R., & Wilson, J. 1973, Physical Review Letters, 31, 1362.
[23] Rueda, J. A., & Ruffini, R. 2012, ApJL, 758, L7.
[24] Sibgatullin, N. R., & Sunyaev, R. A. 2000, Astronomy Letters, 26, 772.
[25] Becerra, L., Cipolletta, F., Fryer, C. L., Rueda, J. A., & Ruffini, R. 2015, ApJ, 812, 100.

The GRB classification scheme [3]

The key recipe: binary systems as progenitors for both long and short bursts!

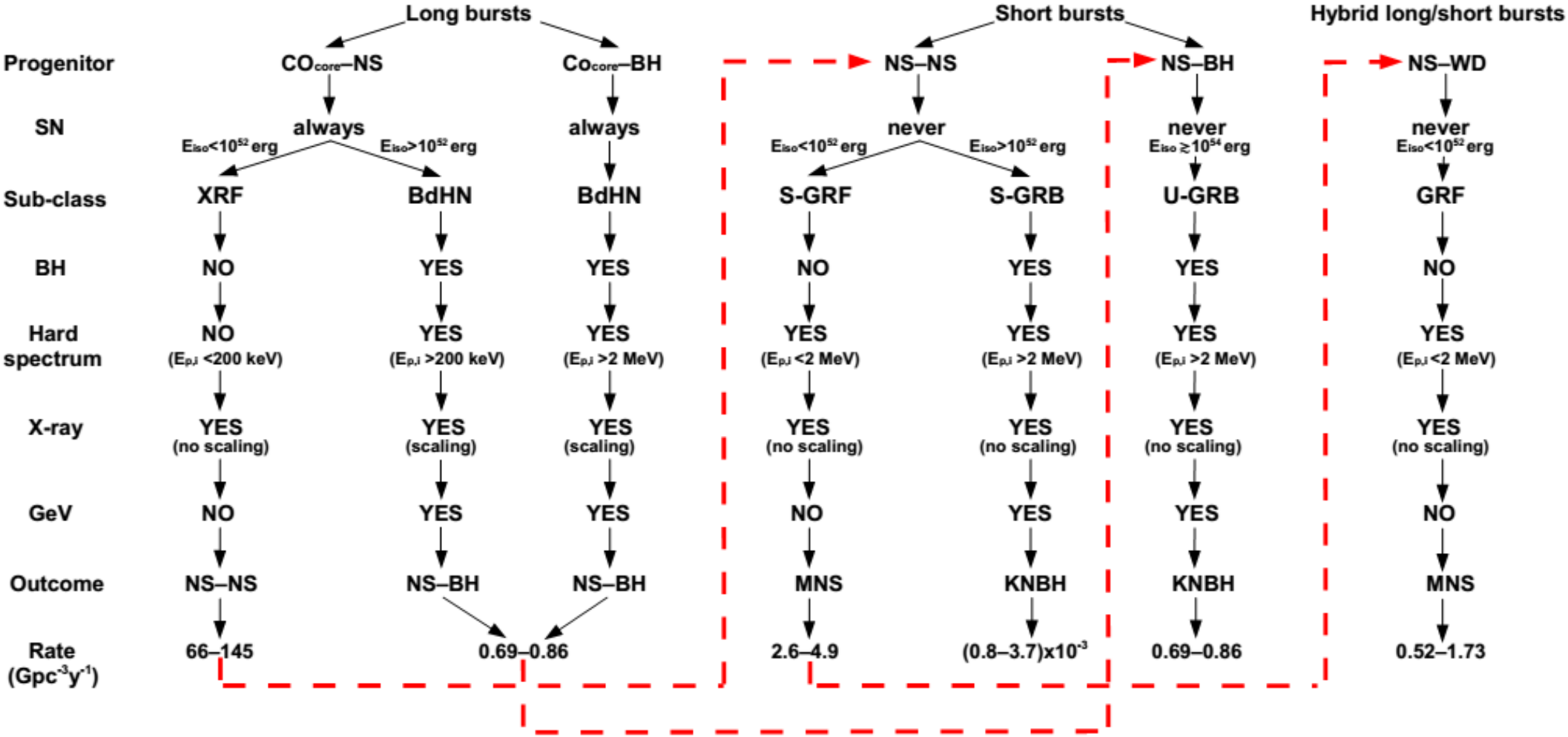

– To date no U-GRBs [26] have been identified and apart them
– only BdHNe (CO_{core}–NS binaries) and S-GRB (NS–NS mergers) harbor BHs,
– GRF have been identified with short bursts with extended emission [27].

[26] Fryer, C. L., Oliveira, F. G., Rueda, J. A., & Ruffini, R. 2015, Physical Review Letters, 115, 231102.
[27] Norris, J. P., & Bonnell, J. T. 2006, ApJ, 643, 266

The GRB classification scheme

Burst T_{90} duration:

Rest-frame **vs** **Observer-frame**

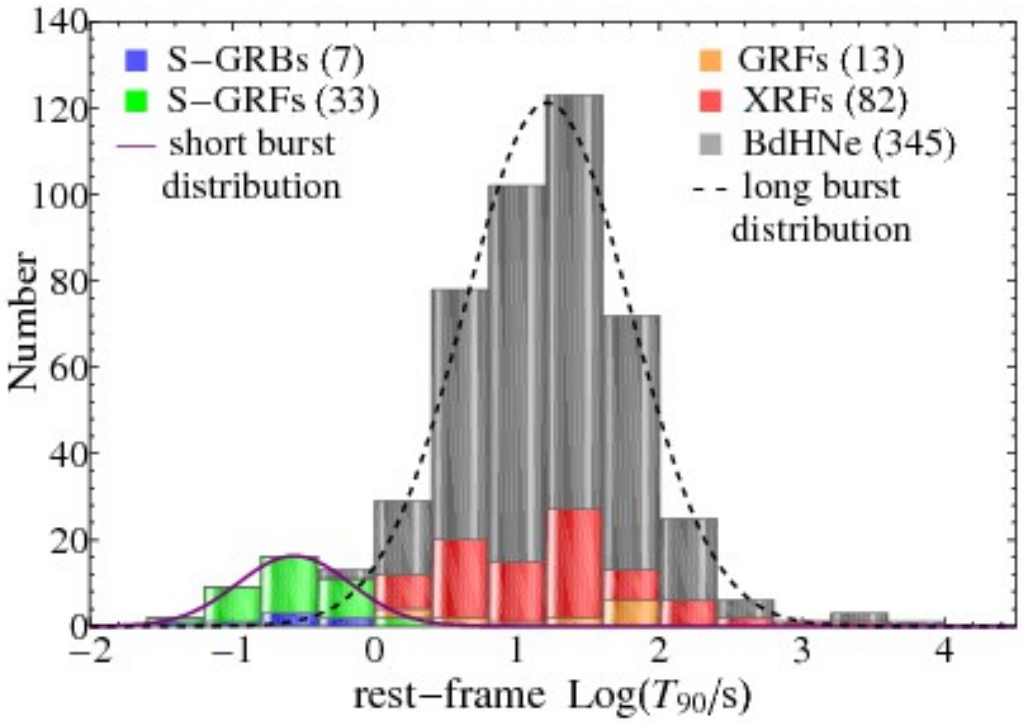

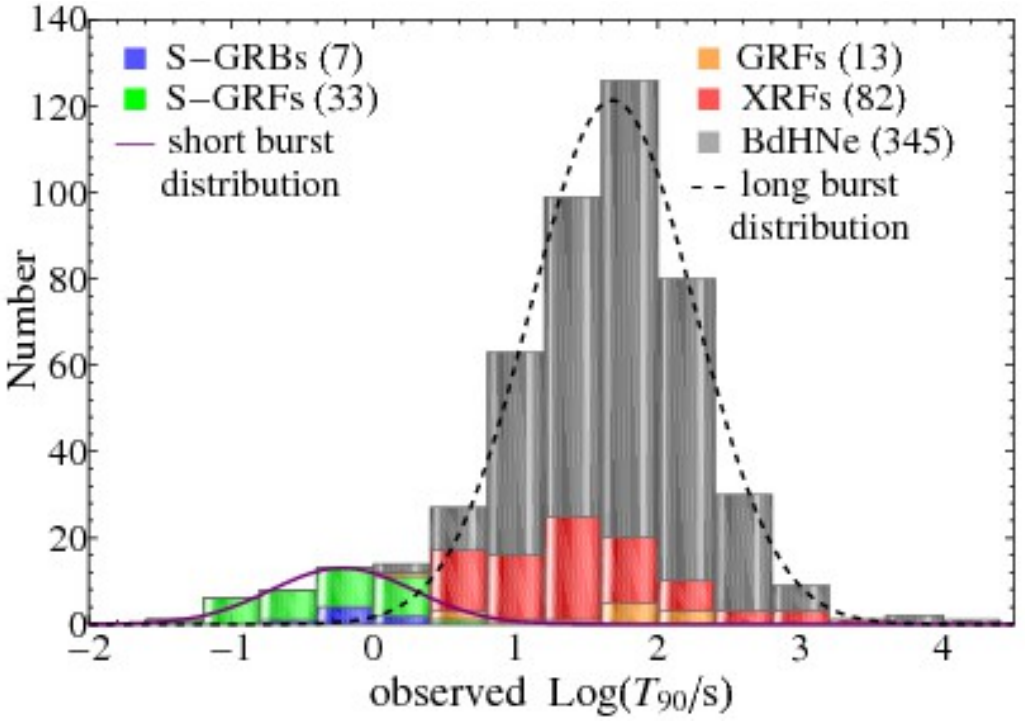

$$T_{90}^{\rm short} = 0.27^{+0.41}_{-0.16}\ {\rm s}$$

$$T_{90}^{\rm long} = 16^{+46}_{-12}\ {\rm s}$$

vs

$$T_{90}^{\rm short} = 0.60^{+1.31}_{-0.41}\ {\rm s}$$

$$T_{90}^{\rm long} = 48^{+133}_{-35}\ {\rm s}$$

Ruffini, R., Wang, Y., Aimuratov, Y., et al 2017, arXiv:170403821

S-GRBs
in the fireshell model

The GRB classification scheme [3]

The key recipe: binary systems as progenitors for both long and short bursts!

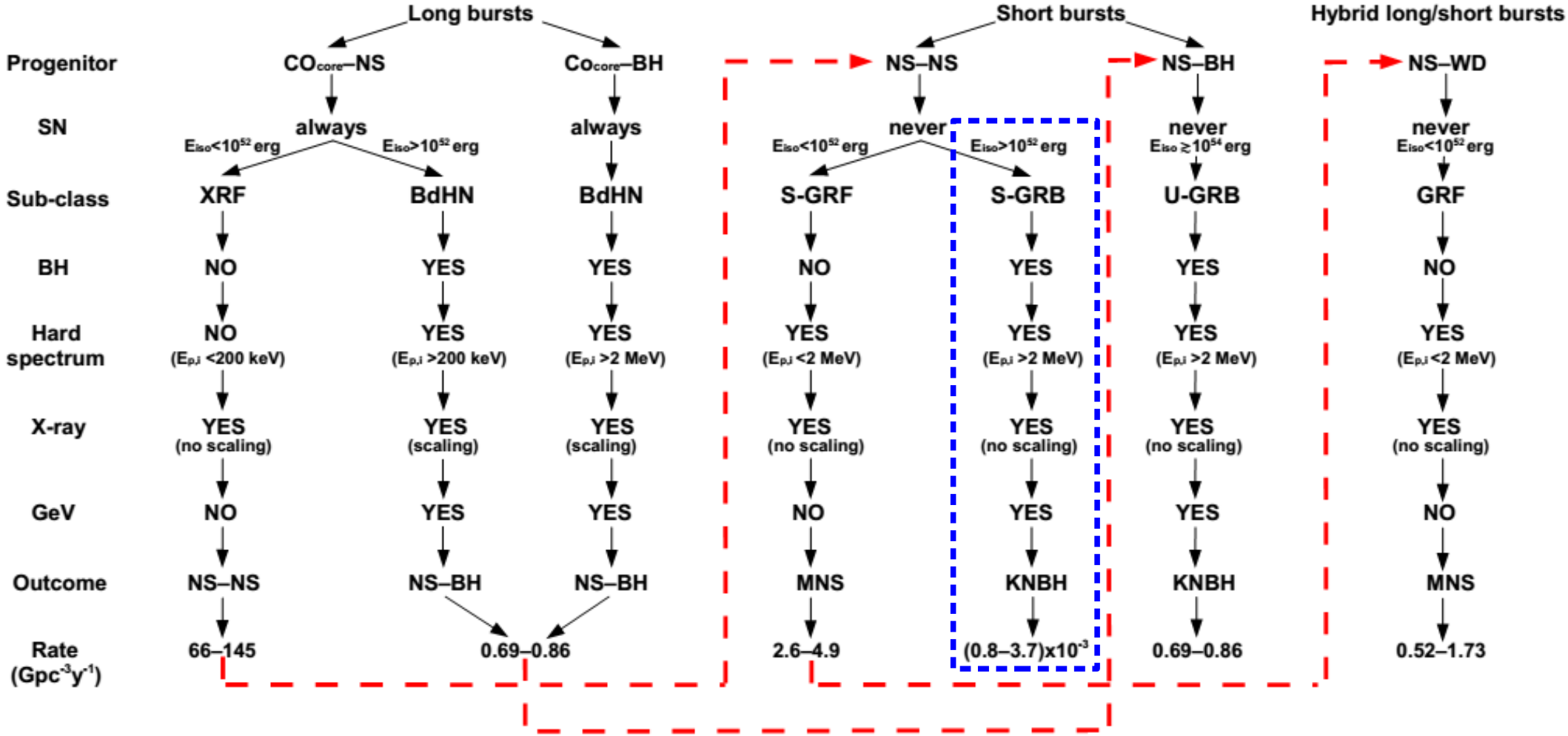

From now on we now focus on S-GRBs which are the only class of observed short GRBs produced in NS–NS mergers leading to the formation of a Kerr BH!

The S-GRBs in the $E_{p,i}$-E_{iso} plane [1–5]

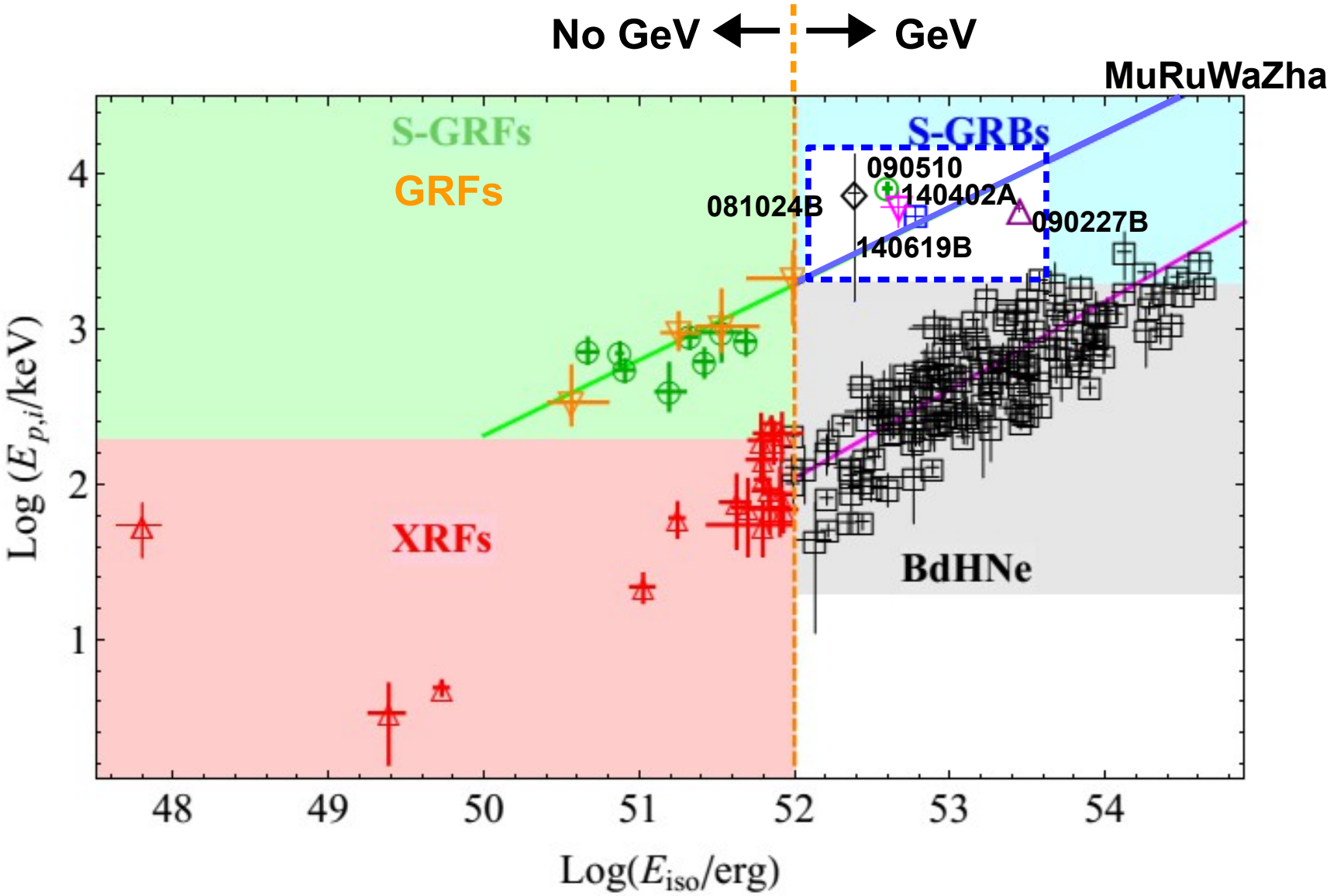

The fireshell model [28–30] and the S-GRBs

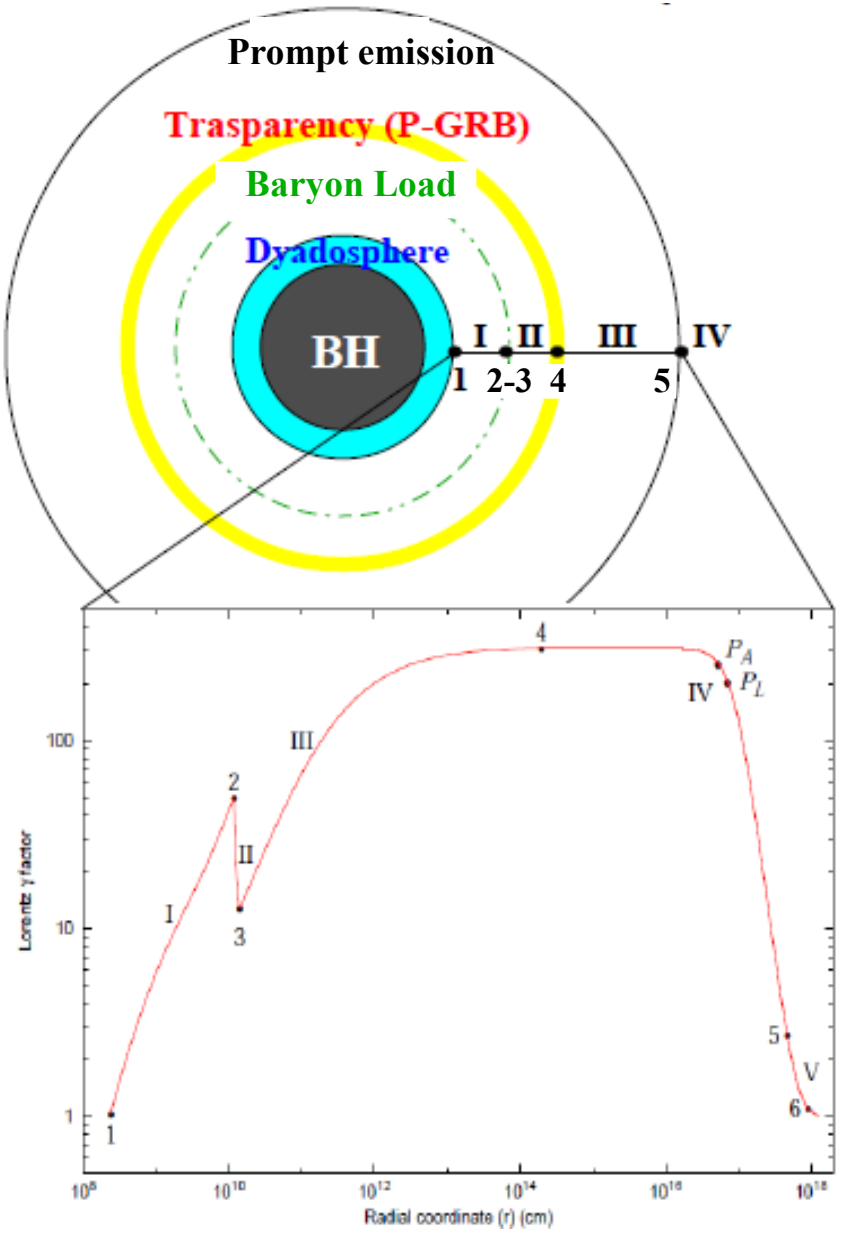

– An optically thick $e^{\pm}$ plasma with energy $E_{\pm}^{tot}$ is formed in the merger of two neutron stars (NS) leading to the birth of a black hole (BH).

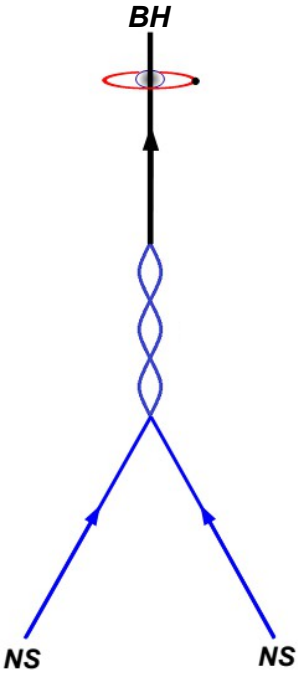

– The expanding $e^{\pm}$ *fireshell* engulfs the baryons left over in the collapse to BH, described by the baryon load $B=M_B c^2/E_{\pm}^{tot}$, and thermalizes with the baryons.

– The fireshell self-accelerates to ultra-relativistic velocities up to the transparency and the Proper-GRB (P-GRB), characterized by a thermal spectrum, is emitted.

– The optically thin shell of baryons collides with a Circum Burst Medium (CBM) of density n_{CBM} giving rise to the prompt emission. The CBM is modeled by the filling factor, which takes into account filamentary structures of the medium, $R=A_{eff}/A_{vis}$.

[28] Ruffini, R., Bianco, C. L., Fraschetti, F., Xue, S., & Chardonnet, P. 2001, ApJ, 555, L117
[29] Ruffini, R., Bianco, C. L., Fraschetti, F., Xue, S., & Chardonnet, P. 2001, ApJ, 555, L113
[30] Ruffini, R., Bianco, C. L., Fraschetti, F., Xue, S., & Chardonnet, P. 2001, ApJ, 555, L107

The space-time diagram of S-GRBs [31]

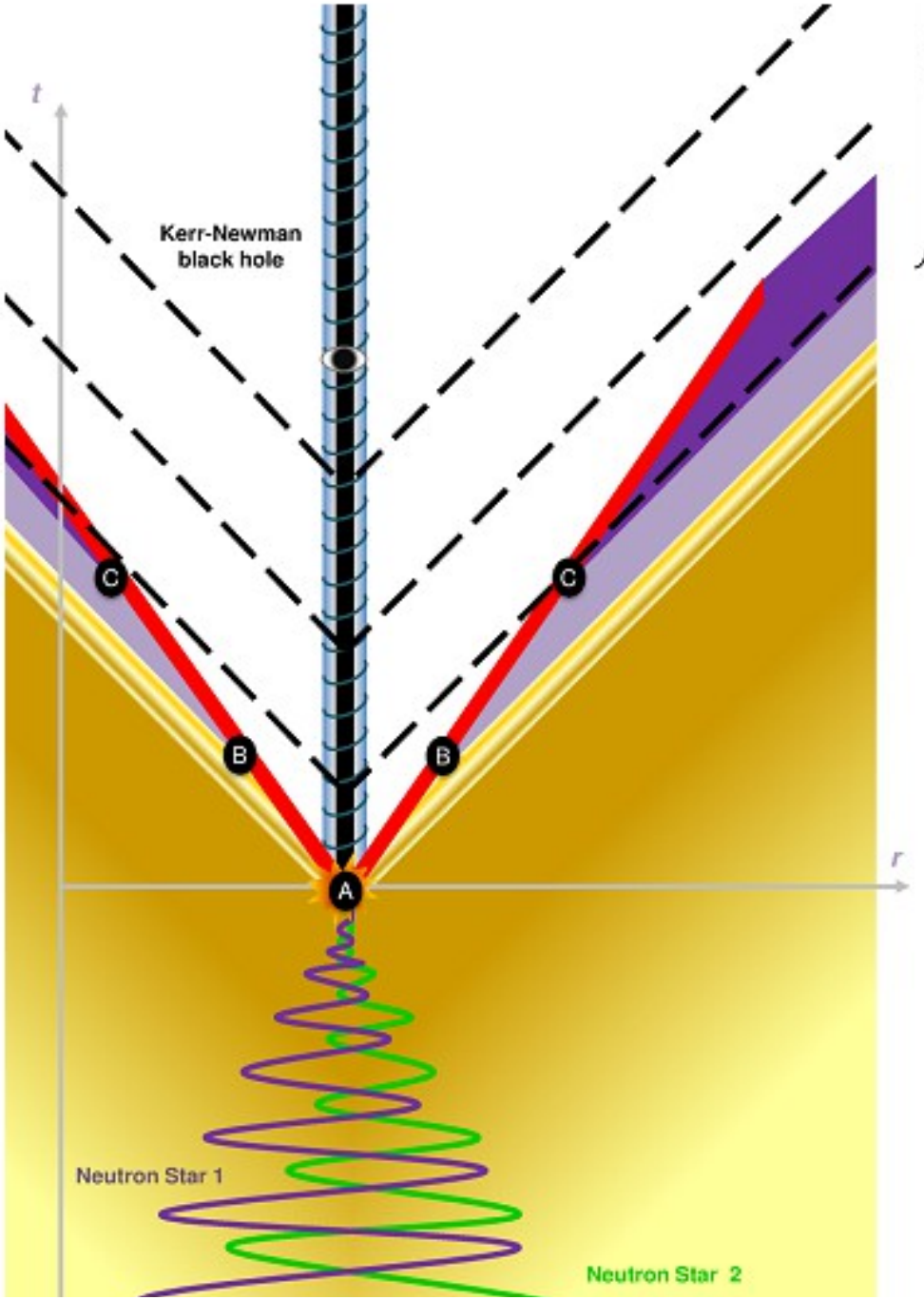

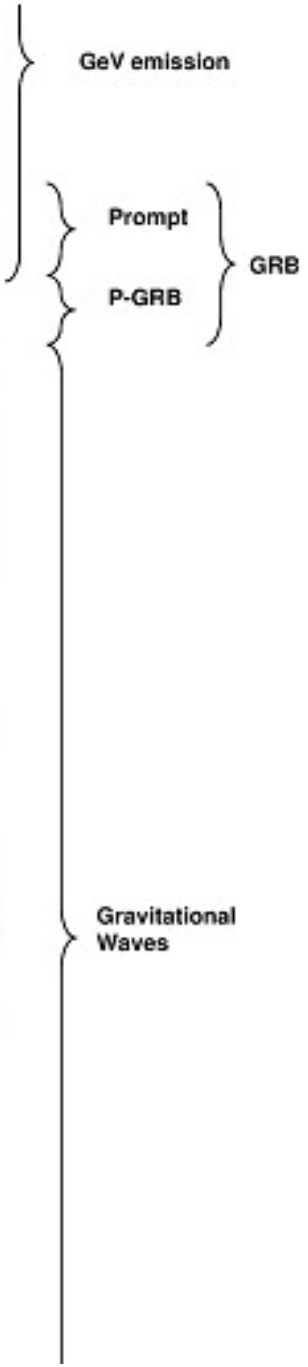

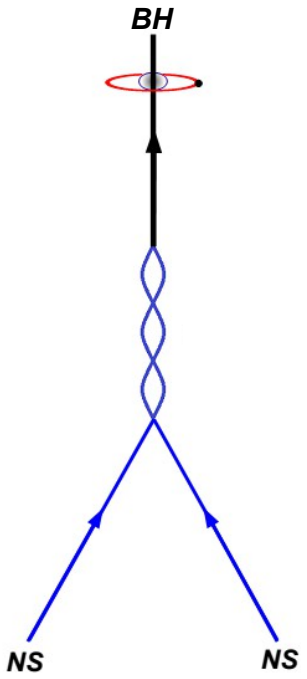

[31] Enderli, M., Bianco, C. L., Izzo, L., et al. 2015, Proceedings of Swift: 10 years of discovery, PoS(SWIFT 10)073

S-GRBs within the fireshell model

S-GRB 090227B

Muccino, M., Ruffini, R., Bianco, et al. 2013,ApJ, 763, 125

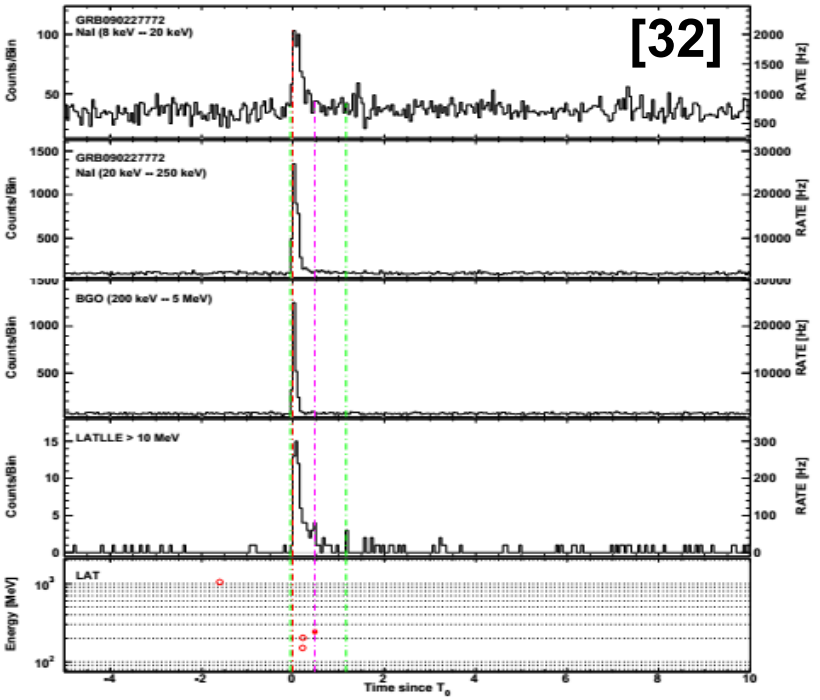

S-GRB 140619B

Ruffini, R., Muccino, M., Kovacevic, M., et al. 2015, ApJ, 808, 19**0**

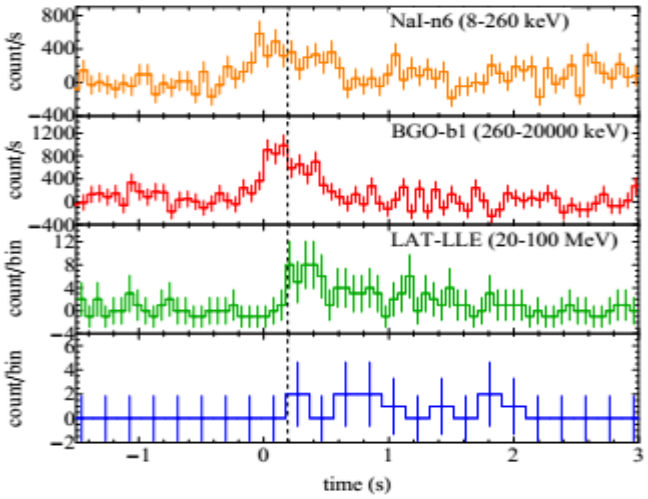

S-GRB 090510

Ruffini, R., et al. 2016, ApJ, 831, 178; arXiv:1607.02400

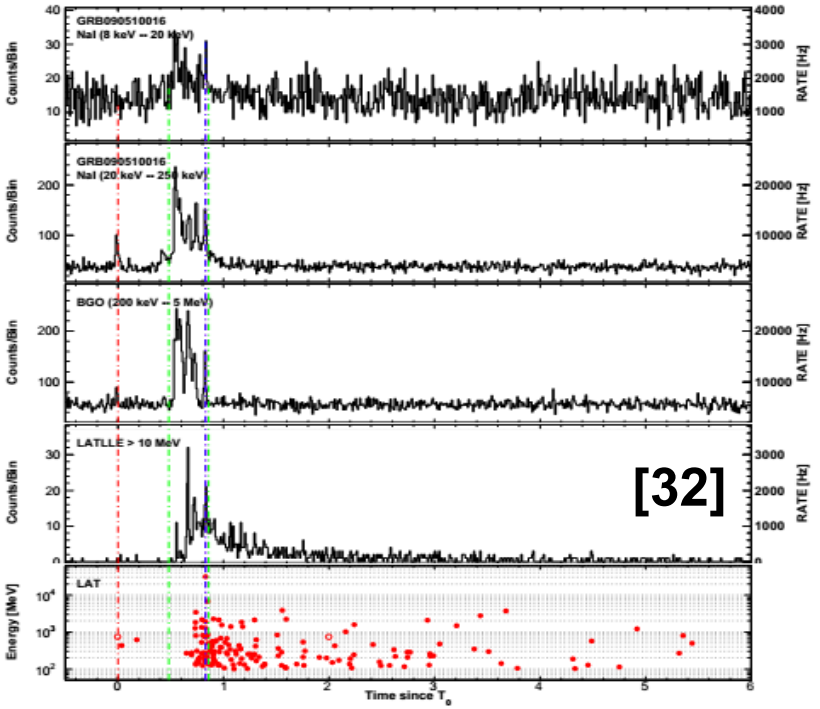

[32] Ackermann, M., Ajello, M., Asano, K., et al. 2013, ApJS, 209, 11

S-GRBs within the fireshell model

S-GRB 081024B

Aimuratov, Y., Ruffini, R., et al., 2017,
ApJ in press; arXiv:170408179

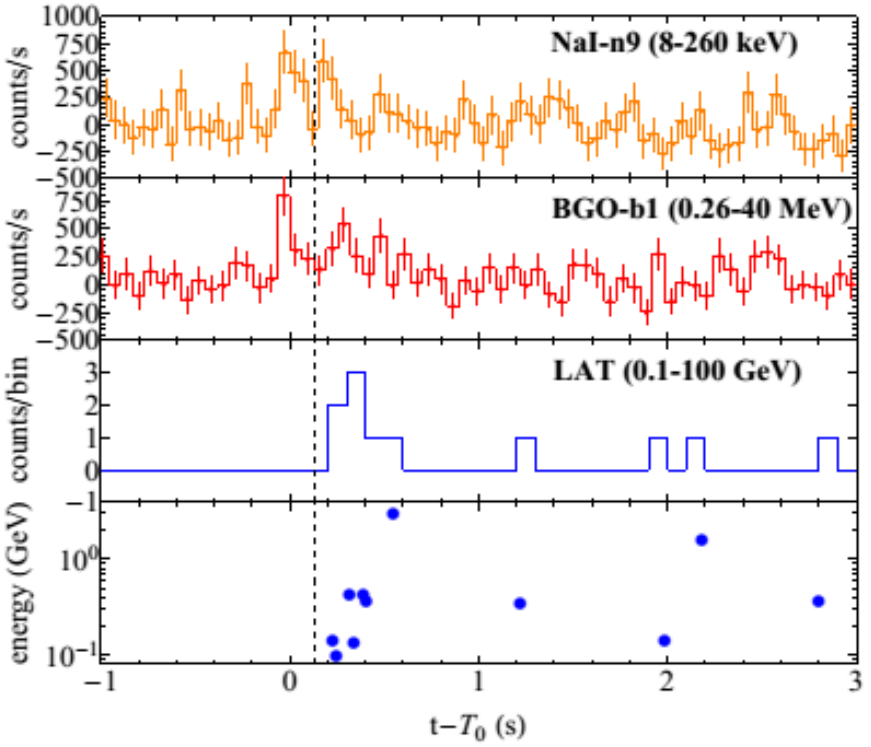

S-GRB 140402A

Aimuratov, Y., Ruffini, R., et al., 2017,
ApJ in press; arXiv:170408179

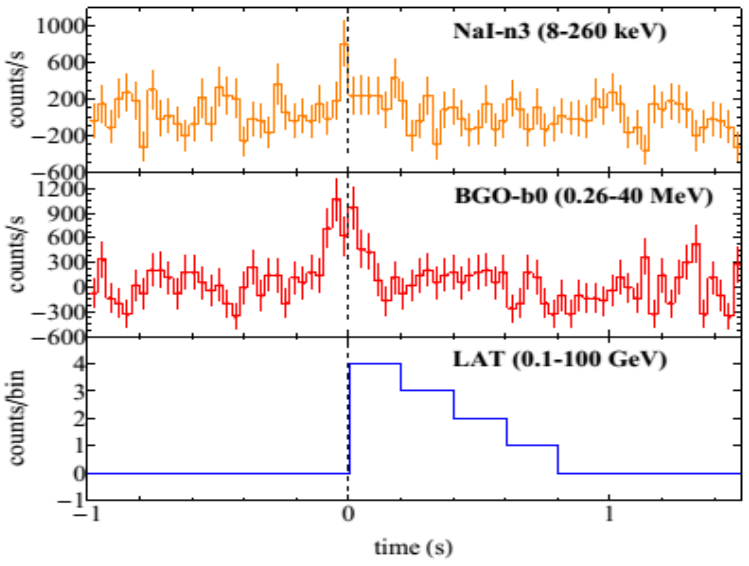

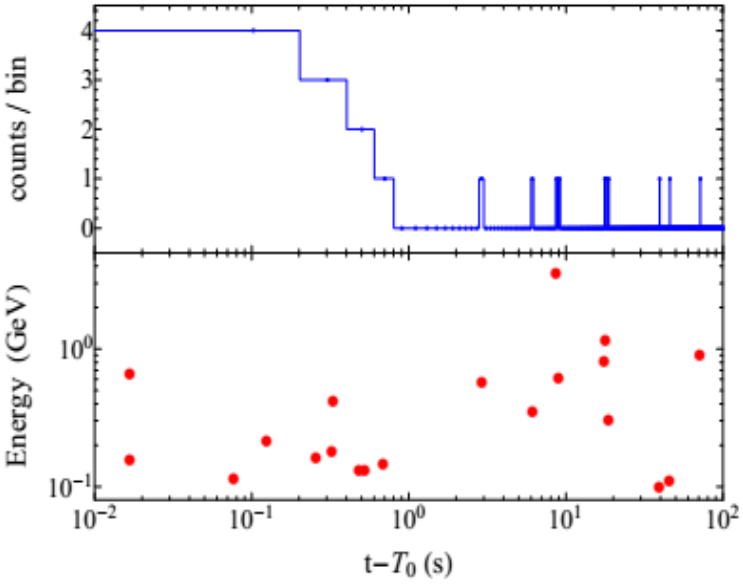

S-GRBs within the fireshell model

S-GRB 090227B

Muccino, M., Ruffini, R., Bianco, et al. 2013,ApJ, 763, 125

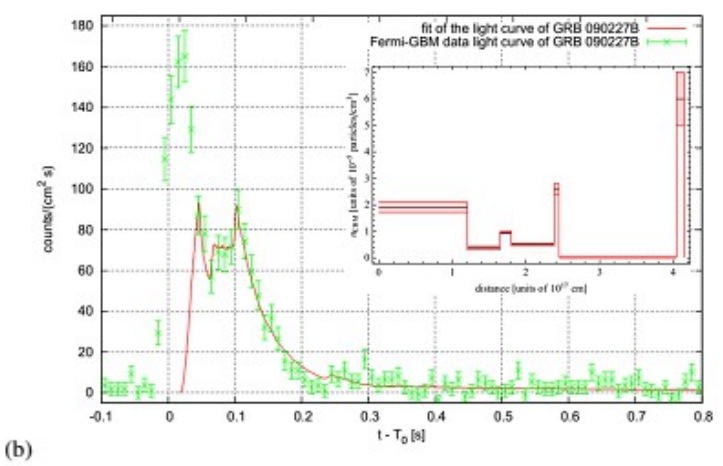

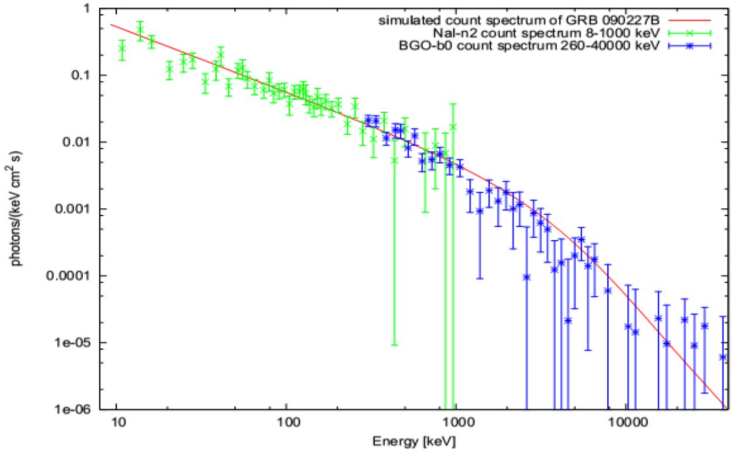

S-GRB 140619B

Ruffini, R., Muccino, M., Kovacevic, M., et al. 2015, ApJ, 808, 19**0**

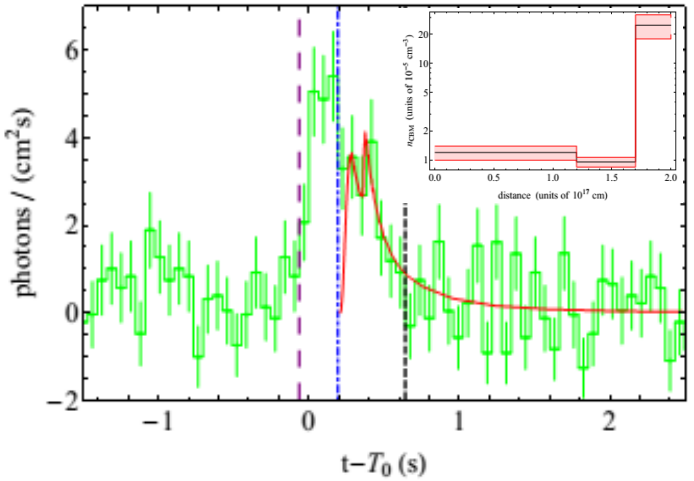

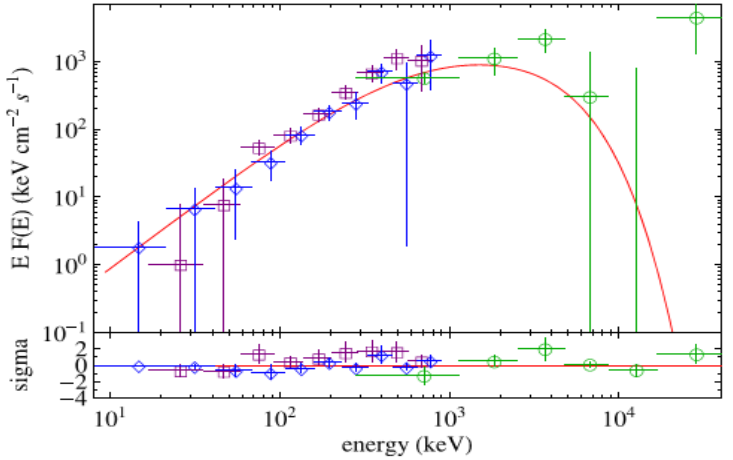

S-GRB 090510

Ruffini, R., et al. 2016, ApJ, 831, 178; arXiv:1607.02400

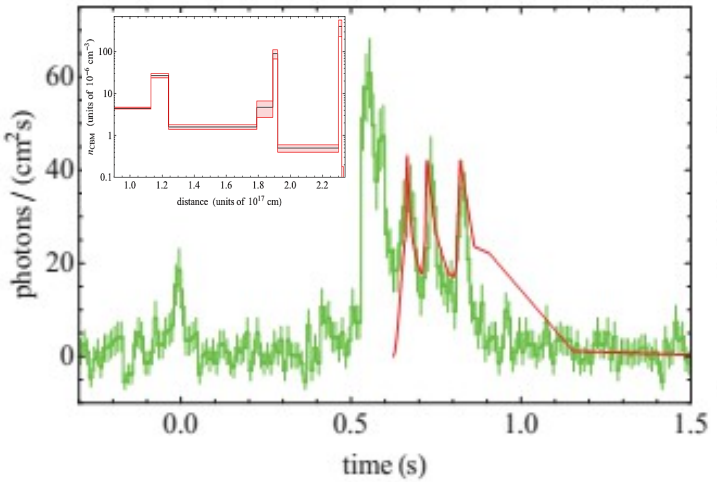

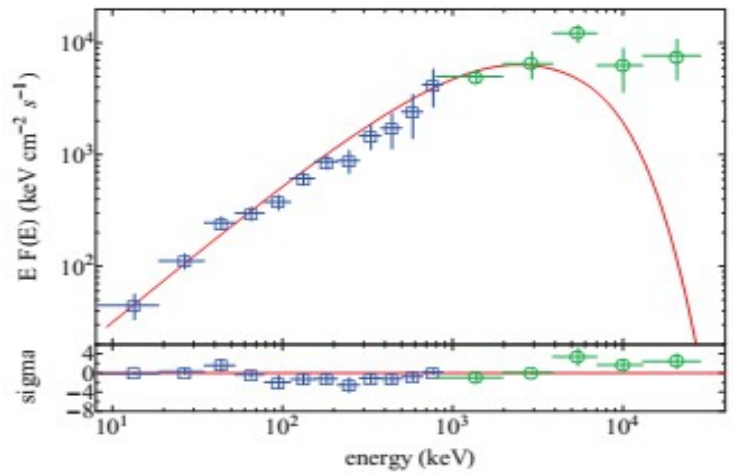

S-GRBs within the fireshell model

S-GRB 081024B

Aimuratov, Y., Ruffini, R., et al., 2017, ApJ in press; arXiv:170408179

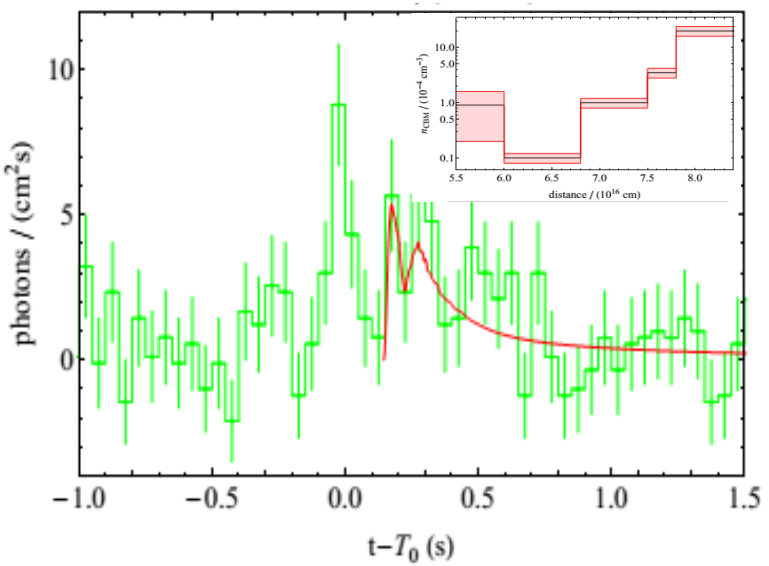

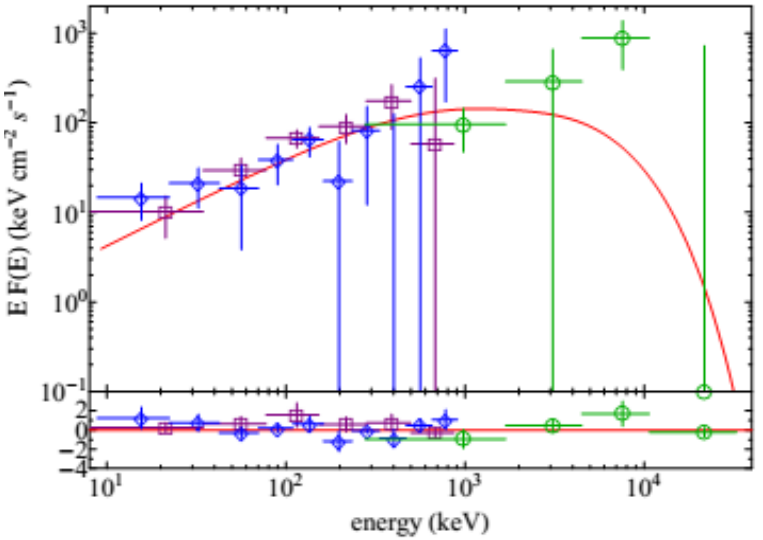

S-GRB 140402A

Aimuratov, Y., Ruffini, R., et al., 2017, ApJ in press; arXiv:170408179

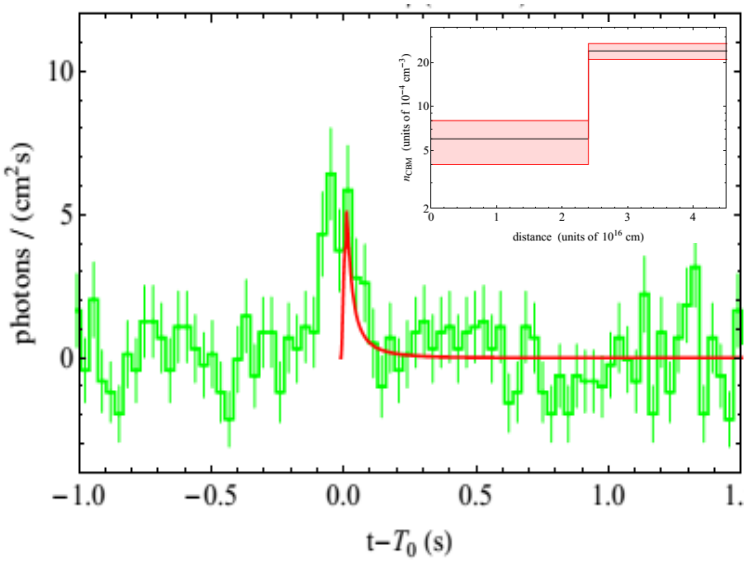

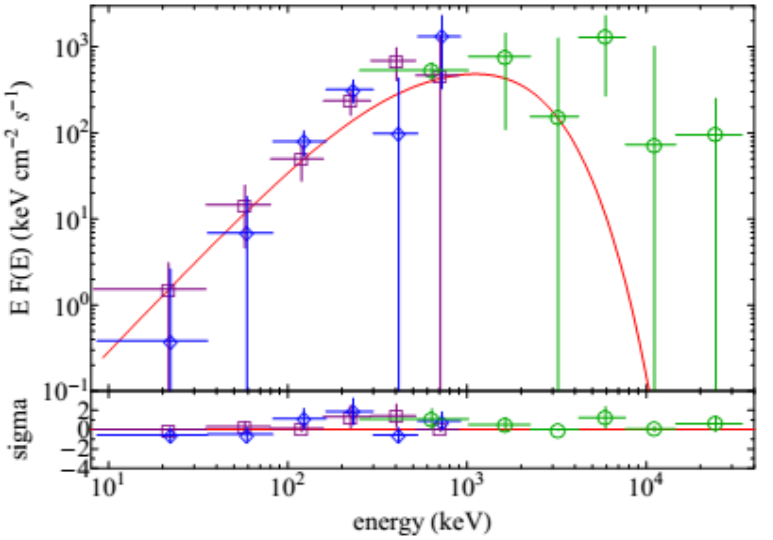

To summarize, all S-GRBs have:

- **B~10^{-5}**
- **$\Gamma \sim 10^4$**
- **$\langle n_{CBM} \rangle \sim 10^{-5}$–$10^{-3}$ cm^{-3}**

The GeV emission in S-GRBs [9]

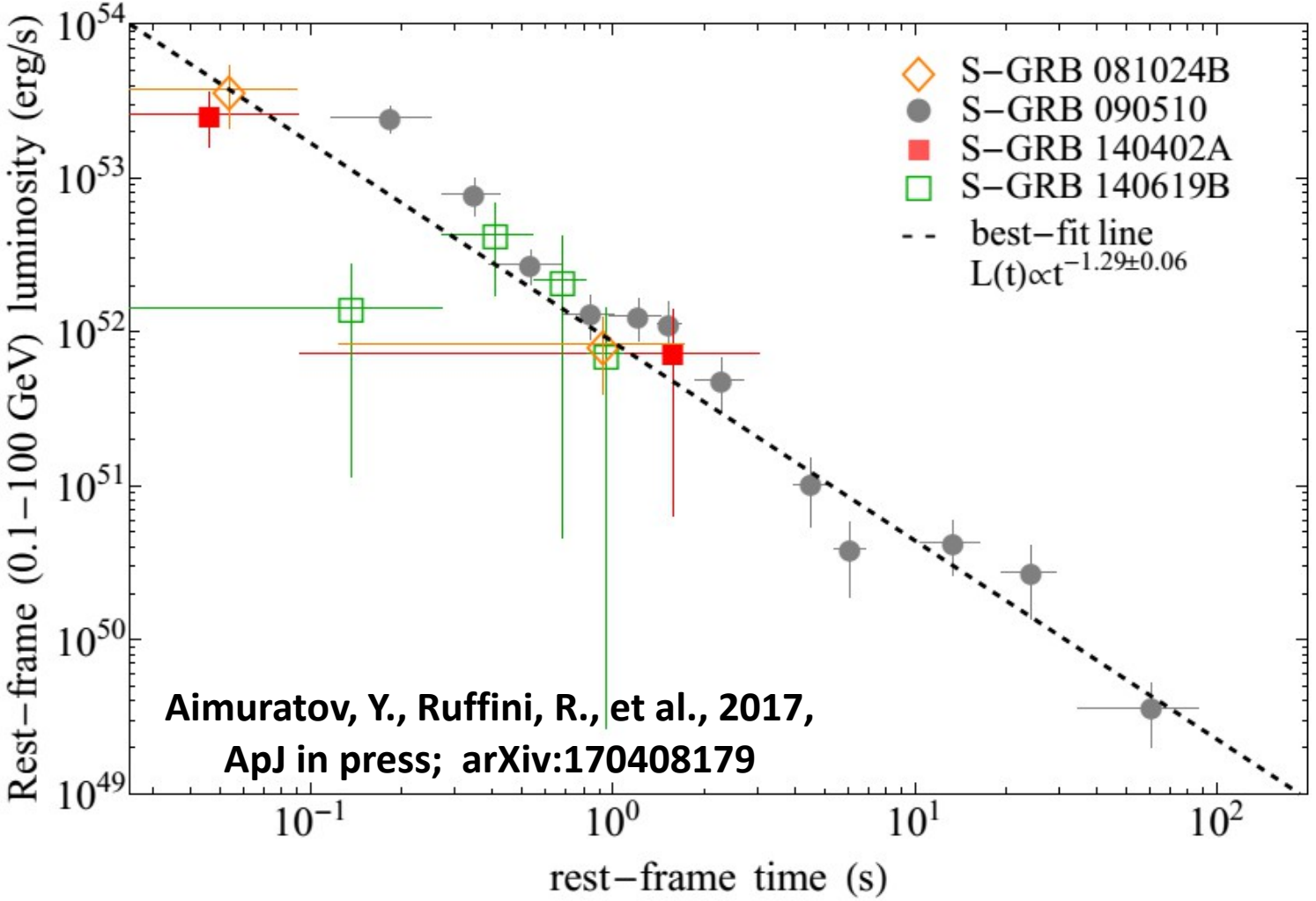

GRB	z	$E_{\rm p,i}$ (MeV)	$E_{\rm iso}$ (10^{52} erg)	$E^{\rm max}_{\rm GeV}$ (GeV)	$\Gamma^{\rm min}_{\rm GeV}$	$E_{\rm LAT}$ (10^{52} erg)	$M^{\eta+}_{\rm acc}$ ($M_\odot$)	$M^{\eta-}_{\rm acc}$ ($M_\odot$)
081024B	3.12 ± 1.82	9.56 ± 4.94	2.64 ± 1.00	3	$\gtrsim 779$	$\gtrsim 2.79 \pm 0.98$	$\gtrsim 0.04$	$\gtrsim 0.41$
090227B	1.61 ± 0.14	5.89 ± 0.30	28.3 ± 1.5	–	–	–	–	–
090510	0.903 ± 0.003	7.89 ± 0.76	3.95 ± 0.21	31	$\gtrsim 551$	$\gtrsim 5.78 \pm 0.60$	$\gtrsim 0.08$	$\gtrsim 0.86$
140402A	5.52 ± 0.93	6.1 ± 1.6	4.7 ± 1.1	3.7	$\gtrsim 354$	$\gtrsim 4.5 \pm 2.2$	$\gtrsim 0.06$	$\gtrsim 0.66$
140619B	2.67 ± 0.37	5.34 ± 0.79	6.03 ± 0.79	24	$\gtrsim 471$	$\gtrsim 2.34 \pm 0.91$	$\gtrsim 0.03$	$\gtrsim 0.35$

The GeV emission in S-GRBs [9]

GRB	z	$E_{\rm p,i}$ (MeV)	$E_{\rm iso}$ (10^{52} erg)	$E^{\rm max}_{\rm GeV}$ (GeV)	$\Gamma^{\rm min}_{\rm GeV}$	$E_{\rm LAT}$ (10^{52} erg)	$M^{\eta+}_{\rm acc}$ ($M_\odot$)	$M^{\eta-}_{\rm acc}$ ($M_\odot$)
081024B	3.12 ± 1.82	9.56 ± 4.94	2.64 ± 1.00	3	$\gtrsim 779$	$\gtrsim 2.79 \pm 0.98$	$\gtrsim 0.04$	$\gtrsim 0.41$
090227B	1.61 ± 0.14	5.89 ± 0.30	28.3 ± 1.5	–	–	–	–	–
090510	0.903 ± 0.003	7.89 ± 0.76	3.95 ± 0.21	31	$\gtrsim 551$	$\gtrsim 5.78 \pm 0.60$	$\gtrsim 0.08$	$\gtrsim 0.86$
140402A	5.52 ± 0.93	6.1 ± 1.6	4.7 ± 1.1	3.7	$\gtrsim 354$	$\gtrsim 4.5 \pm 2.2$	$\gtrsim 0.06$	$\gtrsim 0.66$
140619B	2.67 ± 0.37	5.34 ± 0.79	6.03 ± 0.79	24	$\gtrsim 471$	$\gtrsim 2.34 \pm 0.91$	$\gtrsim 0.03$	$\gtrsim 0.35$

The accretion onto the new-born Kerr BH can explain GeV energy resevoir [8]

$$E_{\rm LAT} = f_{\rm b}^{-1} \eta_{\pm} M_{\rm acc}^{\eta_{\pm}} c^2$$

where $f_b \equiv 1 - \cos\theta$ **and** $\eta_+ = 42.3\%$ **or** $\eta_- = 3.8\%$ **for a Kerr BH [33].**

All S-GRBs, apart the S-GRB 090227B which was outside the nominal LAT FoV, exhibit GeV emission. This suggests that no beaming is necessary in S-GRBs (or that the GeV emission comes from a large angle region), i.e., $f_{\rm b} \equiv 1$ **.**

[33] Ruffini & Wheeler in Landau, L.D. & Lifshitz, E.M. 2003 "The classical theory of fields", 4th revised edition, Butterworth-Heinemann (Oxford), 352

The GeV emission in S-GRBs [9]

GRB	z	$E_{\rm p,i}$ (MeV)	$E_{\rm iso}$ (10^{52} erg)	$E^{\rm max}_{\rm GeV}$ (GeV)	$\Gamma^{\rm min}_{\rm GeV}$	$E_{\rm LAT}$ (10^{52} erg)	$M^{\eta+}_{\rm acc}$ ($M_\odot$)	$M^{\eta-}_{\rm acc}$ ($M_\odot$)
081024B	3.12 ± 1.82	9.56 ± 4.94	2.64 ± 1.00	3	$\gtrsim 779$	$\gtrsim 2.79 \pm 0.98$	$\gtrsim 0.04$	$\gtrsim 0.41$
090227B	1.61 ± 0.14	5.89 ± 0.30	28.3 ± 1.5	–	–	–	–	–
090510	0.903 ± 0.003	7.89 ± 0.76	3.95 ± 0.21	31	$\gtrsim 551$	$\gtrsim 5.78 \pm 0.60$	$\gtrsim 0.08$	$\gtrsim 0.86$
140402A	5.52 ± 0.93	6.1 ± 1.6	4.7 ± 1.1	3.7	$\gtrsim 354$	$\gtrsim 4.5 \pm 2.2$	$\gtrsim 0.06$	$\gtrsim 0.66$
140619B	2.67 ± 0.37	5.34 ± 0.79	6.03 ± 0.79	24	$\gtrsim 471$	$\gtrsim 2.34 \pm 0.91$	$\gtrsim 0.03$	$\gtrsim 0.35$

The accretion onto the new-born Kerr BH can explain GeV energy resevoir [8]

$$E_{\rm LAT} = f_{\rm b}^{-1} \eta_{\pm} M_{\rm acc}^{\eta_{\pm}} c^2$$

where $f_b \equiv 1 - \cos\theta$ **and** $\eta_+ = 42.3\%$ **or** $\eta_- = 3.8\%$ **for a Kerr BH [33].**

All S-GRBs, apart the S-GRB 090227B which was outside the nominal LAT FoV, exhibit GeV emission. This suggests that no beaming is necessary in S-GRBs (or that the GeV emission comes from a large angle region), i.e., $f_{\rm b} \equiv 1$ **.**

From the pair production optical depth formula [34], for the GeV emission we infer $\Gamma^{\rm min}_{\rm GeV} \gtrsim 300$**: the outflow from the new-born BH is ultrarelativistic.**

[33] Ruffini & Wheeler in Landau, L.D. & Lifshitz, E.M. 2003 "The classical theory of fields", 4th revised edition, Butterworth-Heinemann (Oxford), 352
[34] Lithwick, Y., & Sari, R., 2001, ApJ, 555, 540

The GeV emission in S-GRBs [9]

GRB	z	$E_{\rm p,i}$ (MeV)	$E_{\rm iso}$ (10^{52} erg)	$E^{\rm max}_{\rm GeV}$ (GeV)	$\Gamma^{\rm min}_{\rm GeV}$	$E_{\rm LAT}$ (10^{52} erg)	$M^{\eta+}_{\rm acc}$ ($M_\odot$)	$M^{\eta-}_{\rm acc}$ ($M_\odot$)
081024B	3.12 ± 1.82	9.56 ± 4.94	2.64 ± 1.00	3	$\gtrsim 779$	$\gtrsim 2.79 \pm 0.98$	$\gtrsim 0.04$	$\gtrsim 0.41$
090227B	1.61 ± 0.14	5.89 ± 0.30	28.3 ± 1.5	–	–	–	–	–
090510	0.903 ± 0.003	7.89 ± 0.76	3.95 ± 0.21	31	$\gtrsim 551$	$\gtrsim 5.78 \pm 0.60$	$\gtrsim 0.08$	$\gtrsim 0.86$
140402A	5.52 ± 0.93	6.1 ± 1.6	4.7 ± 1.1	3.7	$\gtrsim 354$	$\gtrsim 4.5 \pm 2.2$	$\gtrsim 0.06$	$\gtrsim 0.66$
140619B	2.67 ± 0.37	5.34 ± 0.79	6.03 ± 0.79	24	$\gtrsim 471$	$\gtrsim 2.34 \pm 0.91$	$\gtrsim 0.03$	$\gtrsim 0.35$

The accretion onto the new-born Kerr BH can explain GeV energy resevoir [8]

$$E_{\rm LAT} = f_{\rm b}^{-1} \eta_{\pm} M_{\rm acc}^{\eta_{\pm}} c^2$$

where $f_b \equiv 1 - \cos\theta$ **and** $\eta_+ = 42.3\%$ **or** $\eta_- = 3.8\%$ **for a Kerr BH [33].**

All S-GRBs, apart the S-GRB 090227B which was outside the nominal LAT FoV, exhibit GeV emission. This suggests that no beaming is necessary in S-GRBs (or that the GeV emission comes from a large angle region), i.e., $f_{\rm b} \equiv 1$ **.**

From the pair production optical depth formula [34], for the GeV emission we infer $\Gamma^{\rm min}_{\rm GeV} \gtrsim 300$**: the outflow from the new-born BH is ultrarelativistic.**

The standard behavior of the GeV luminosity and values of the accreted mass points to a commonality in the mass and spin of the new-born BH in all S-GRBs.

[33] Ruffini & Wheeler in Landau, L.D. & Lifshitz, E.M. 2003 "The classical theory of fields", 4th revised edition, Butterworth-Heinemann (Oxford), 352
[34] Lithwick, Y., & Sari, R., 2001, ApJ, 555, 540

X-ray emission in S-GRBs [9]

GRB 090510 is the only S-GRB with an observed X-ray afterglow. We use its X-ray afterglow as a template for the other S-GRBs.

We deal with 3 redshift transformations:

1) rest-frame energy band

$$0.3\left(\frac{1+z_{\rm fin}}{1+z_{\rm in}}\right)-10\left(\frac{1+z_{\rm fin}}{1+z_{\rm in}}\right)\ {\rm keV}$$

2) flux

$$f^{\rm fin}_{\rm obs}=f^{\rm in}_{\rm obs}\left[\frac{d_{\rm l}(z_{\rm in})}{d_{\rm l}(z_{\rm fin})}\right]^2\frac{\int_{0.3\frac{1+z_{\rm fin}}{1+z_{\rm in}}\,{\rm keV}}^{10\frac{1+z_{\rm fin}}{1+z_{\rm in}}\,{\rm keV}}N(E)EdE}{\int_{0.3\,{\rm keV}}^{10\,{\rm keV}}N(E)EdE}=$$

$$=f^{\rm in}_{\rm obs}\left[\frac{d_{\rm l}(z_{\rm in})}{d_{\rm l}(z_{\rm fin})}\right]^2\left(\frac{1+z_{\rm fin}}{1+z_{\rm in}}\right)^{2-\gamma}.$$

3) time dilation

$$t_{\rm fin}=\left(\frac{1+z_{\rm fin}}{1+z_{\rm in}}\right)t_{\rm in}$$

There is no evidence in favor/against a common behavior of the X-ray afterglow of S-GRBs.

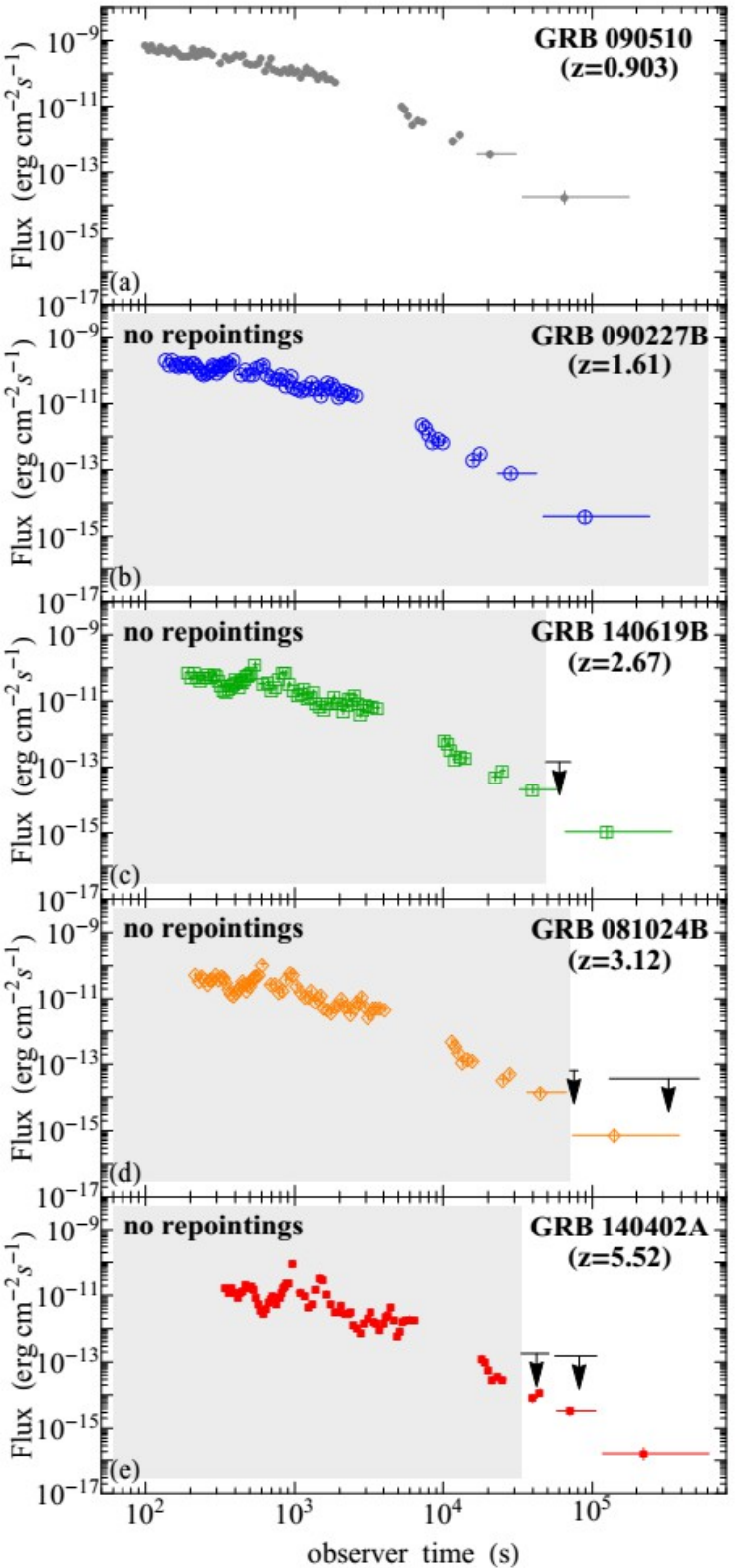

[9] Aimuratov, Y., Ruffini, R., et al., 2017, ApJ in press; arXiv:170408179

The emission in gravitational waves (GW) [35]

Summary of the observational properties of the 7 different burst sub-classes [3]

	Sub-class	In-state	Out-state	$E_{p,i}$ (MeV)	E_{iso} (erg)	$E_{iso,X}$ (erg)	$E_{iso,Gev}$ (erg)	z_{max}	ρ_{GRB} (Gpc^{-3}yr^{-1})
I	XRFs	CO_{core}-NS	νNS-NS	$\lesssim 0.2$	$\sim 10^{48}$–10^{52}	$\sim 10^{48}$–10^{51}	–	1.096	100^{+45}_{-34}
II	BdHNe	CO_{core}-NS	νNS-BH	~ 0.2–2	$\sim 10^{52}$–10^{54}	$\sim 10^{51}$–10^{52}	$\lesssim 10^{53}$	9.3	$0.77^{+0.09}_{-0.08}$
III	BH-SN	CO_{core}-BH	νNS-BH	$\gtrsim 2$	$> 10^{54}$	$\sim 10^{51}$–10^{52}	$\gtrsim 10^{53}$	9.3	$\lesssim 0.77^{+0.09}_{-0.08}$
IV	S-GRFs	NS-NS	MNS	$\lesssim 2$	$\sim 10^{49}$–10^{52}	$\sim 10^{49}$–10^{51}	–	2.609	$3.6^{+1.4}_{-1.0}$
V	S-GRBs	NS-NS	BH	$\gtrsim 2$	$\sim 10^{52}$–10^{53}	$\lesssim 10^{51}$	$\sim 10^{52}$–10^{53}	5.52	$\left(1.9^{+1.8}_{-1.1}\right) \times 10^{-3}$
VI	U-GRBs	νNS-BH	BH	$\gtrsim 2$	$> 10^{52}$	–	–	–	$\gtrsim 0.77^{+0.09}_{-0.08}$
VII	GRFs	NS-WD	MNS	~ 0.2–2	$\sim 10^{51}$–10^{52}	$\sim 10^{49}$–10^{50}	–	2.31	$1.02^{+0.71}_{-0.46}$

GW properties from the merger of the progenitors of short bursts [35]

	ΔE_{insp} (erg)	ΔE_{merger} (erg)	f_{merger} (kHz)	f_{qnm} (kHz)	z^{obs}_{min}	$d_{L_{min}}$ (Mpc)	d_{GW} (Mpc) O1	d_{GW} (Mpc) 2022+
S-GRF	7.17×10^{52}	1.60×10^{53}	1.20	3.84	0.111	508.70	168.43	475.67
S-GRB	1.02×10^{53}	2.28×10^{53}	1.43	2.59	0.903	5841.80	226.62	640.18
U-GRB	1.02×10^{53}	2.03×10^{52}	0.98	2.30	0.169	804.57	235.62	665.72
U-GRB (BH-SN)	1.34×10^{53}	1.35×10^{53}	0.38	0.90	0.169	804.57	362.27	1023.43

[35] Ruffini, R., Rodriguez, J., Muccino, M., Rueda, J. A., et al. 2016, arXiv:160203545

GRB rates vs aLIGO detections [35]

How many aLIGO detections are expected from the inferred GRB local rates?

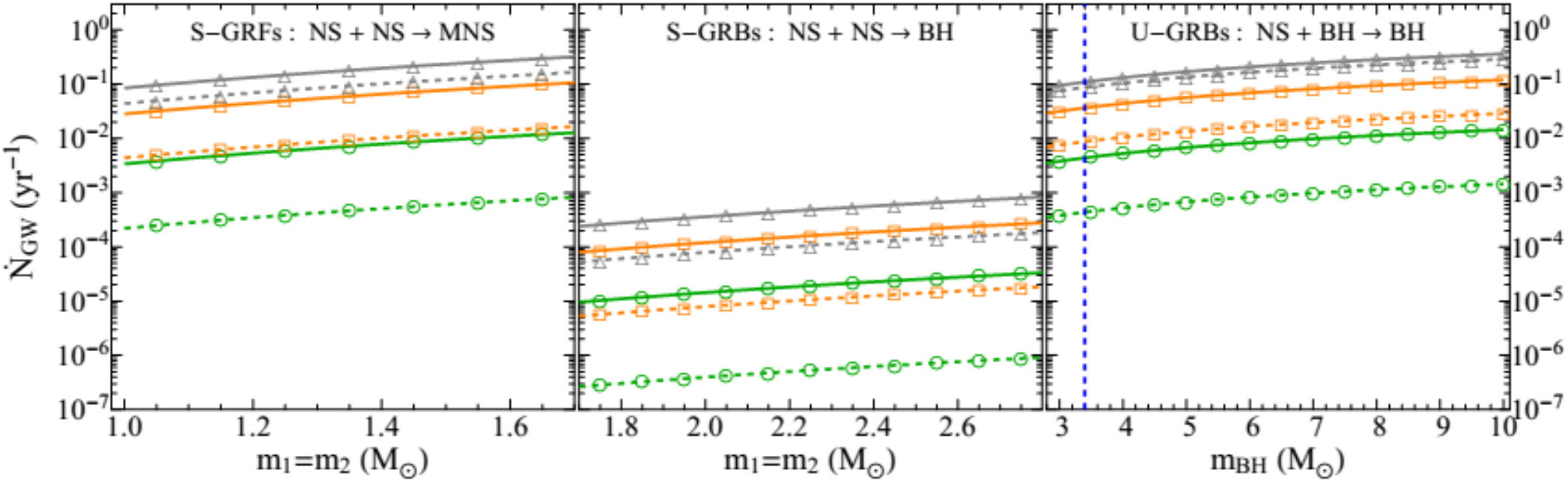

GRB sub-class	$\dot{N}_{GRB}$ (yr^{-1})	$\dot{N}^{obs}_{GRB} = N^{obs}_{GRB}/T_{obs}$ (yr^{-1})	$\dot{N}_{GW} = \rho_{GRB} V^{GW}_{max}$ (yr^{-1})
XRFs	144–733	1 (1997–2014)	undetectable
BdHNe	662–1120	14 (1997–2014)	undetectable
BH-SN	$\lesssim$ 662–1120	$\lesssim$ 14 (1997–2014)	undetectable
S-GRFs	58–248	3 (2005–2014)	O1: $(0.4–8)\times10^{-3}$ O3: 0.011–0.065 2022+: 0.1–0.2
S-GRBs	2–8	1 (2006–2014)	O1: $(0.4–8)\times10^{-6}$ O3: $(0.08–1.2)\times10^{-4}$ 2022+: $(0.8–3.6)\times10^{-4}$
U-GRBs	662–1120	–	O1: $(0.36–3.6)\times10^{-3}$ O3: 0.008–0.032 2022+: 0.076–0.095
U-GRBs (BH-SN)	$\lesssim$ 662–1120	–	O1: 0.0016–0.016 O3: $\lesssim$ 0.029–0.12 2022+: $\lesssim$ 0.3–0.36
GRFs	29-153	1 (2005–2014)	undetectable

[35] Ruffini, R., Rodriguez, J., Muccino, M., Rueda, J. A., et al. 2016, arXiv:160203545

Amplitude vs sensitivity

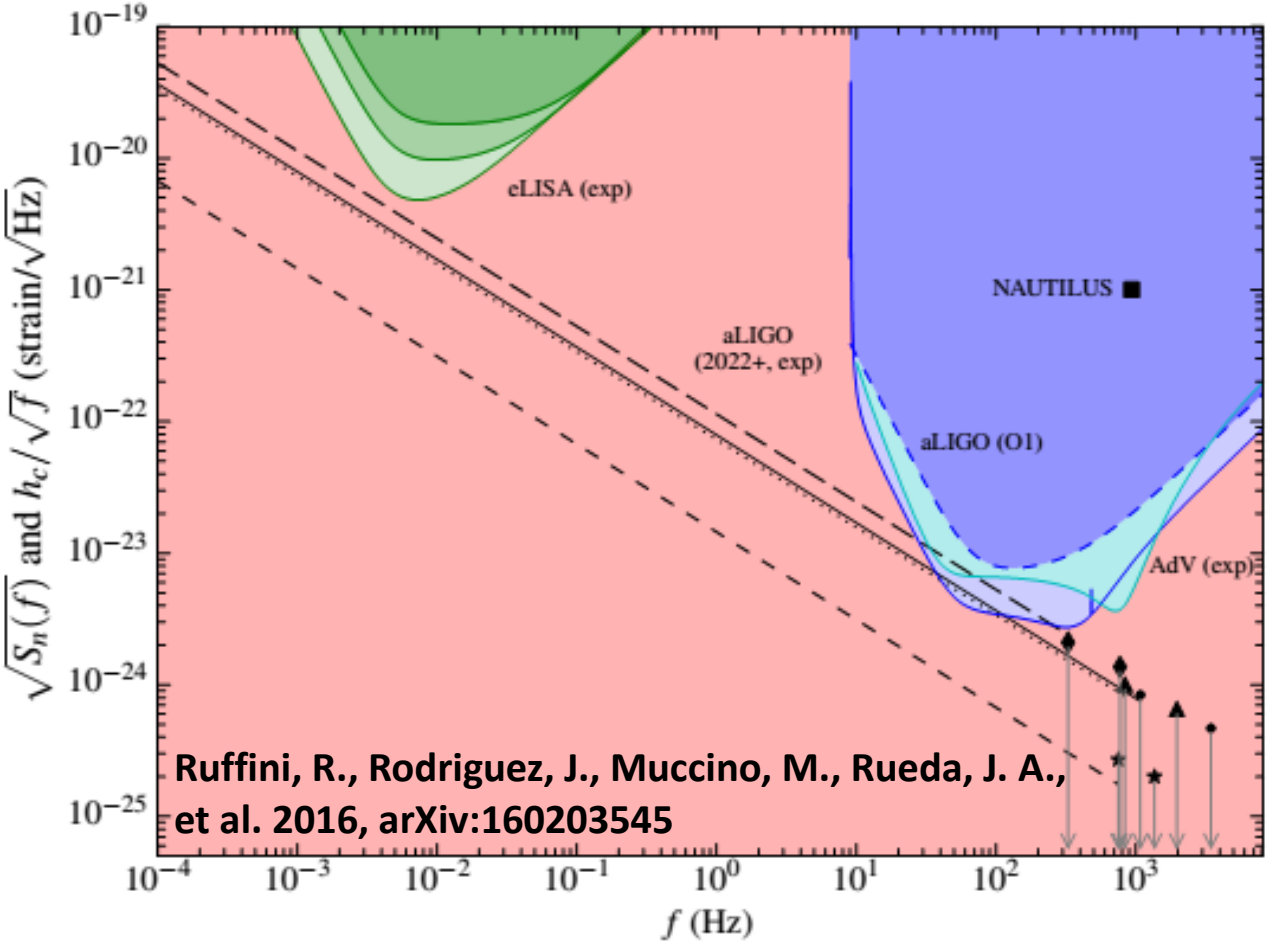

Figure 1. Comparison of the signal's ASD $h_c/\sqrt{f}$ of S-GRFs, S-GRBs and U-GRBs with the noise's ASD $\sqrt{S_n(f)}$, where S_n is the power spectrum density of the detector's noise of eLISA, of aLIGO and of the bar detector NAUTILUS. The green lines, from top to bottom, are the expected noise's ASD of the N2A1, N2A2 and N2A5 configurations of eLISA (Klein et al. 2016). The dashed and continuous blue lines correspond to the noise's ASD respectively of aLIGO O1 run (2015/2016) and of the expected aLIGO 2022+ run (Abbott et al. 2016), and the cyan line is the expected noise's ASD of AdV (BNS-optimized; Abbott et al. 2016). The filled square indicates the noise's ASD of the NAUTILUS resonant bar for a 1 ms GW burst (Astone et al. 2006, 2008). The red filled area indicates the region of undetectability by any of the above instruments. We recall that in this plot the GW frequency is redshifted by a factor $1+z$ with respect to the source frame value, i.e. $f = f_s/(1+z)$, for which we use the cosmological redshift and corresponding luminosity distance of the closest observed source of each sub-class (see Table 2). The following three curves correspond to the inspiral regime of the coalescence: S-GRFs with $(1.4+1.4)\ M_\odot$ (solid curve), S-GRBs with $(2.0+2.0)\ M_\odot$ (short-dashed curve), U-GRB with $(1.5+3.0)\ M_\odot$ (dotted curve) from *out-states* of BdHNe, and U-GRB with $(1.5+10.0)\ M_\odot$ (long dashed curve) from *out-states* of BH-SNe. The dot, star, triangle and diamond correspond to h_c in the merger regime for S-GRFs, S-GRBs, U-GRBs from *out-states* of BdHNe, and U-GRBs from *out-states* of BH-SNe, respectively. The first point is located at $f_{\rm merger}/(1+z)$ and the second at $f_{\rm qnm}/(1+z)$ (see Table 2). The down-arrows indicate that these estimates have to be considered as upper limits since we have assumed that all the energy release in the system goes in GWs, which clearly overestimates the GW energy output in view of the dominance of the electromagnetic emission (see Table 3). We have also overestimated the GW energy in the merger regime by using Eq. (9) which is the expected GW energy emitted in the plunge+merger+ringdown phases of a BH-BH merger. For binary mergers involving NSs, as we have discussed in Sec. 2.3, the energy released in GWs must be necessarily lower than this value.

Conclusions

⟹ All bursts originate from binary systems. Among the observed sources only BdHNe (CO_{core}–NS binaries) and S-GRB (NS–NS mergers) harbor BHs.

⟹ All S-GRBs have similar values of the baryon load, the Lorentz factor at transparency and the CBM density, i.e., $B \sim 10^{-5}$, $\Gamma \sim 10^{4}$, $\langle nCBM \rangle \sim 10^{-5}$–$10^{-3}$ cm^{-3}.

⟹ All S-GRBs within the Fermi-LAT FoV exhibit GeV emission. Therefore no beaming is necessary to explain the ultrarelativistic GeV emission ($\Gamma^{\rm min}_{\rm GeV} \gtrsim 300$) and starts after the P-GRB emission. This points to the fact that this emission originates from the on-set of the BH formation.

⟹ The common power-law behavior of S-GRB GeV luminosities points to a common mass and spin of the new-born BH and is in line with the expected NS mass in binaries and the range of the NS critical mass 2.2–2.7 M_{sun} .

⟹ The GeV energy can be explained by the accretion of $M \approx 0.03$–0.08 M_{sun} (or $M \approx 0.35$–0.86 M_{sun}) for co- (or counter) rotating around an extreme Kerr BH. This can harbor also r-process (Ruffini et al. 2014; Becerra et al. 2016).

⟹ GWs might be detectable for S-GRBS at $z \leq 0.14$ by the aLIGO 2022+ run. All S-GRBs are at $z \geq 0.903$, thus no GWs can be detected from these sources.

Thank you

Local rate estimates

Taking into account the observational constraints, i.e., the detector solid angle coverage of the sky and sensitivities, which define a maximum volume of observation depending on the intrinsic luminosity of the sources, we compute the local rates following Ref. [25]

$$\rho_0 \simeq \sum_i \sum_{\log L_{\min}}^{\log L_{\max}} \frac{4\pi}{\Omega_i T_i} \frac{1}{\ln 10} \frac{1}{g(L)} \frac{\Delta N_i}{\Delta \log L} \frac{\Delta L}{L},$$

where $g(L) = \int_0^{z_{\max}(L)} \frac{f(z)}{1+z} \frac{dV(z)}{dz} dz$ **and** $\frac{dV(z)}{dz} = \frac{c}{H_0} \frac{4\pi d_L^2}{(1+z)^2 [\Omega_M (1+z)^3 + \Omega_\Lambda]^{1/2}}$

Ruffini et al. 2016 ApJ, 832, 136

LITERATURE

- **XRFs:** $\rho_0 = 100^{+45}_{-34}\,\mathrm{Gpc^{-3}\ y^{-1}}$ → $164^{+98}_{-65}\,\mathbf{Gpc^{-3}\ y^{-1}}$ [a]
- **BdHNe: (U-GRBs)** $\rho_0 = 0.77^{+0.09}_{-0.08}\ \mathrm{Gpc^{-3}\ y^{-1}}$ → $1.3^{+0.6}_{-0.7}\,\mathbf{Gpc^{-3}\ y^{-1}}$ [b]; $0.8^{+0.1}_{-0.1}\,\mathbf{Gpc^{-3}\ y^{-1}}$ [a]
- **S-GRFs:** $\rho_0 = 3.6^{+1.4}_{-1.0}\ \mathrm{Gpc^{-3}\ y^{-1}}$
- **S-GRBs:** $\rho_0 = \left(1.9^{+1.8}_{-1.1}\right) \times 10^{-3}\ \mathrm{Gpc^{-3}\ y^{-1}}$ → $4.1^{+2.3}_{-1.9}\,\mathbf{Gpc^{-3}\ y^{-1}}$ [c]; $4.2^{+1.3}_{-1.0}, 3.9^{+1.2}_{-0.9}, 7.1^{+2.2}_{-1.7}\,\mathbf{Gpc^{-3}\ y^{-1}}$ [a]
- **GRFs:** $\rho_0 = 1.02^{+0.71}_{-0.46}\ \mathrm{Gpc^{-3}\ y^{-1}}$ **NEW!**

[a] Sun, H., Zhang, B., & Li, Z. 2015, ApJ, 812, 33
[b] Wanderman, D., & Piran, T. 2010, MNRAS, 406, 1944
[c] Wanderman, D., & Piran, T. 2015, MNRAS, 448, 3026

A particular BdHN: GRB 110731A

(Daria Primorac's talk)

Does GRB 110731A belong to the BdHNe?

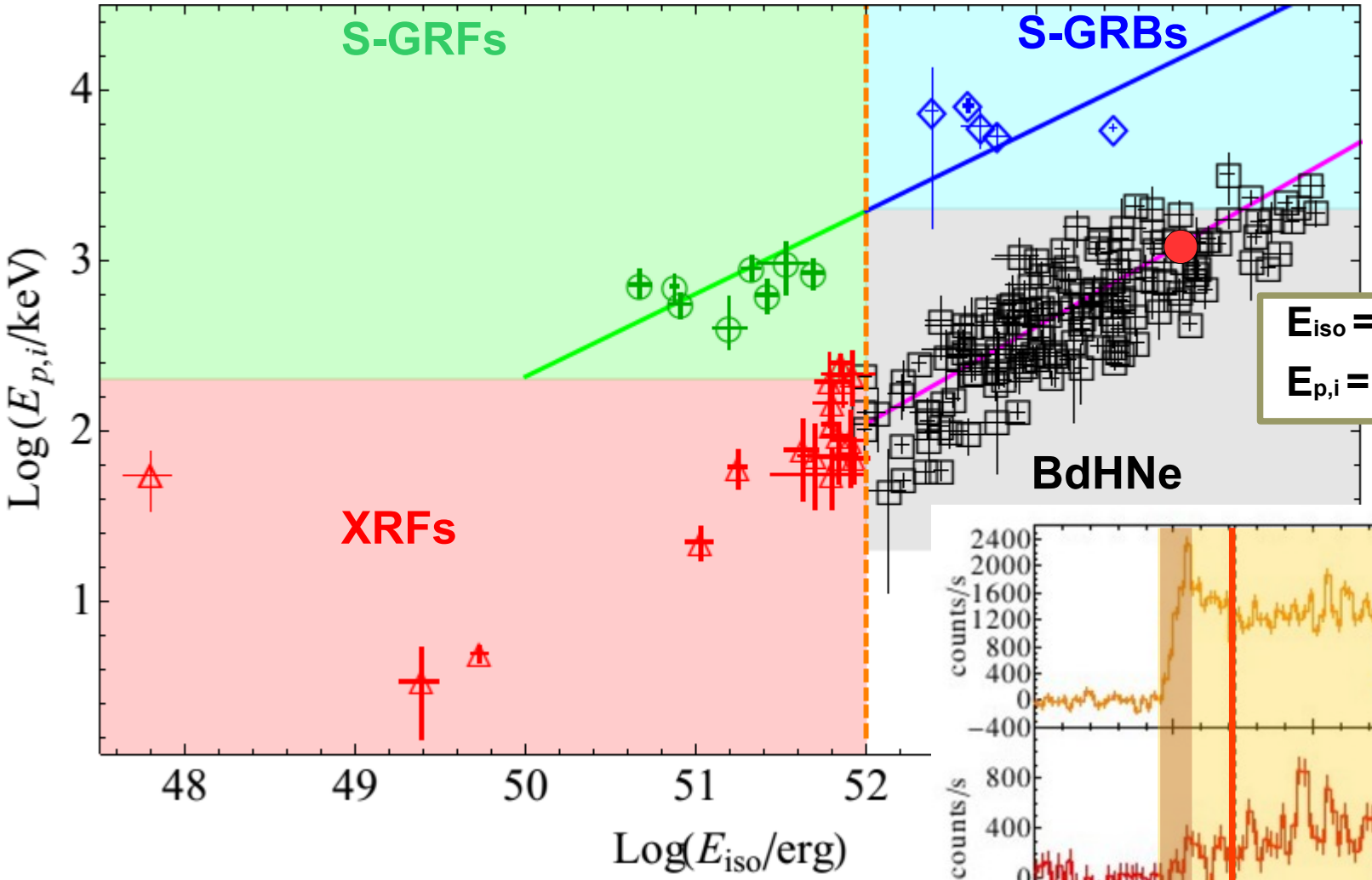

$E_{iso} = (6.05 \pm 0.09) \times 10^{53}$ erg

$E_{p,i} = 1231$ keV

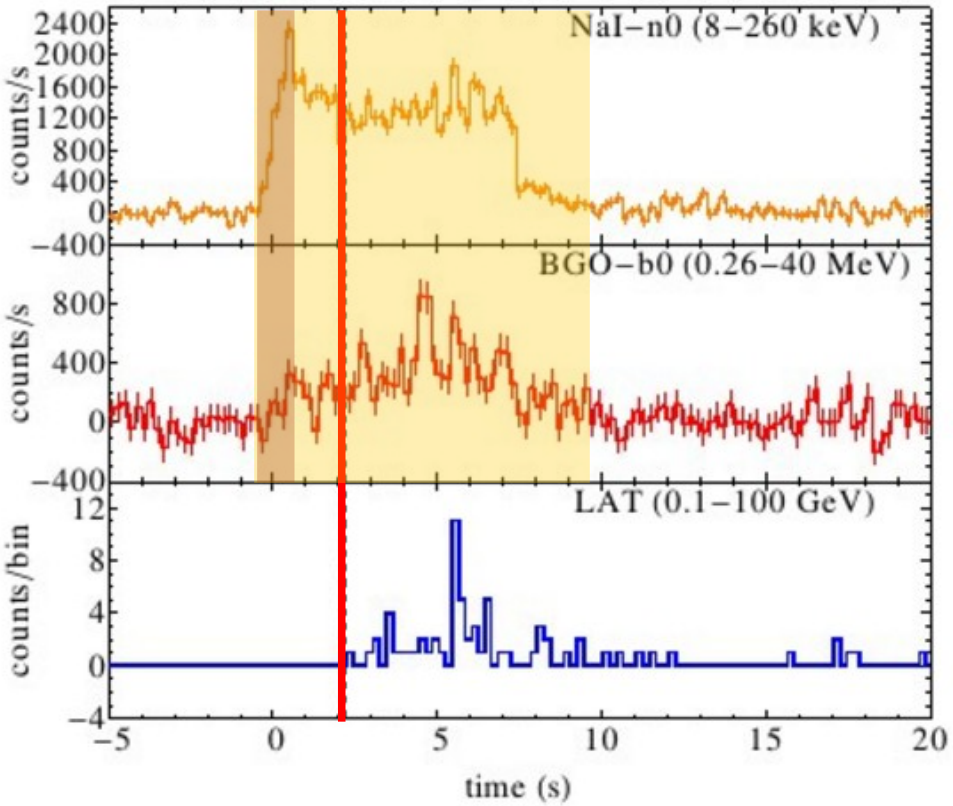

Does GRB 110731A belong to the BdHNe?

1) **EPISODE 1: not detected in view of the compactness of the CO_{core}–NS progenitor**

2) **EPISODE 2: fireshell simulation**

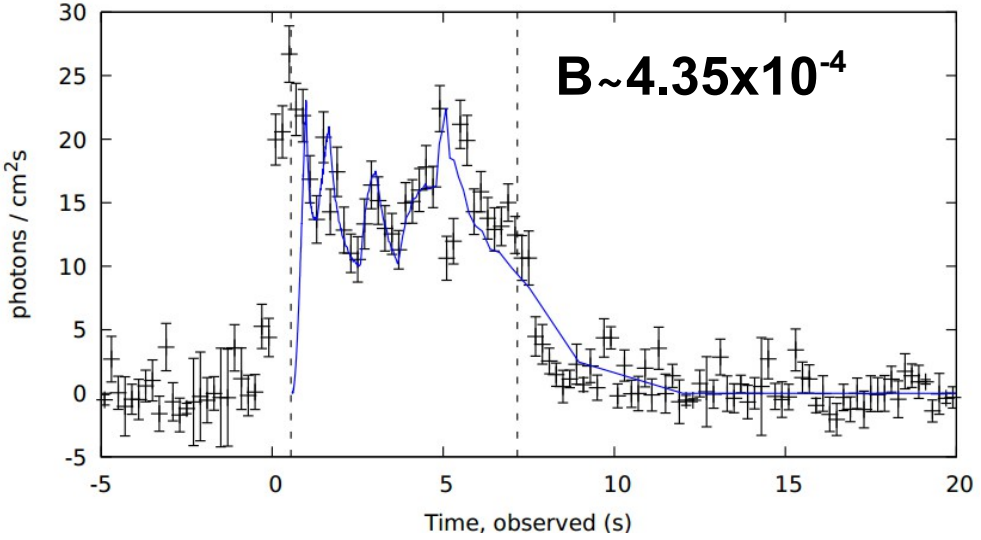

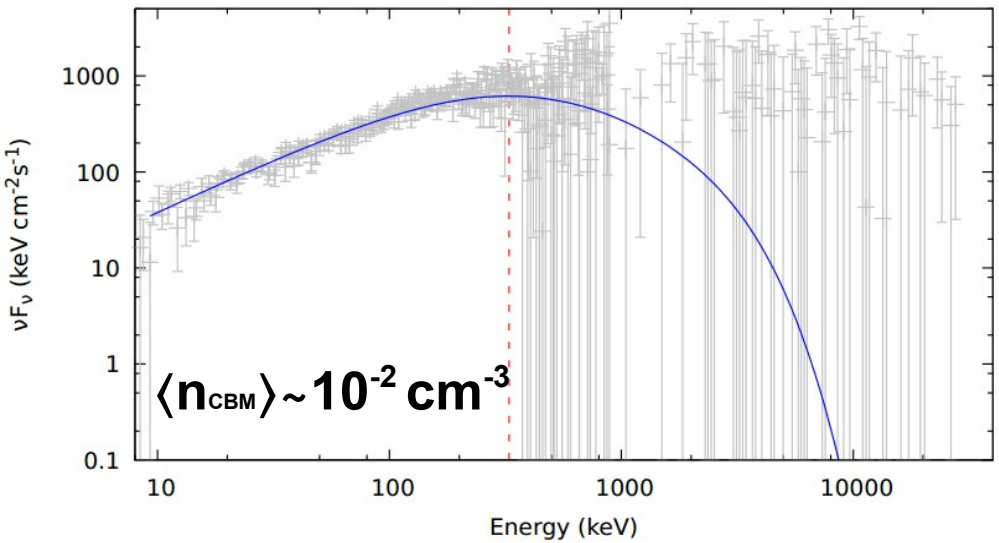

3) **FPA: typical scaling law but no flare, nor plateau**

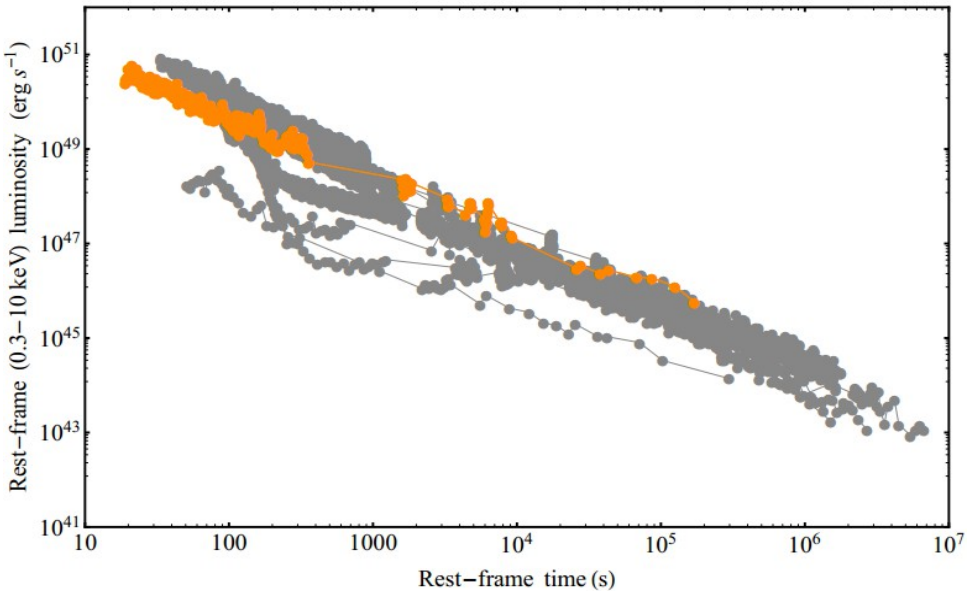

4) **GeV emission: typical of BdHNe**